UNIVERSITY OF CALIFORNIA SAN DIEGO

Investigating the Role of K63-linked Polyubiquitination in Oncogenic IKKβ and BRAF Mutants

A thesis submitted in partial satisfaction of the
requirements for the degree Master of Science

in

Chemistry

by

Guillermo Cardenas

Committee in charge:

Professor Daniel J. Donoghue, Chair
Professor Galia Debelouchina
Professor Judy Kim

2018

The Thesis of Guillermo Cardenas is approved, and is acceptable in quality and form for publication on microfilm and electronically:

_____

_____

_____

Chair

University of California San Diego

2018

DEDICATION

To my parents, my family, and my friends

for their love and their continued support throughout my college career.

TABLE OF CONTENTS

LIST OF FIGURES

ACKNOWLEDGEMENTS

This work would not have been possible without Dan Donoghue and all the members of the lab. As my PI, Dan has taught me the invaluable skill on how to be a proper researcher, and I would like to thank you for your guidance and support throughout my program, as well as bearing with my experimental mishaps. I would like to thank April Meyer for her advice and guidance in lab. Without her advice on troubleshooting, I would have no doubt taken twice as long. I would also like to thank all the members of the lab for their support, especially Leo Gallo and Juyeon Ko for pioneering these projects and for their advice on future directions.

Chapter 1, in full, has been submitted for publication as it may appear in PLOS one, Meyer AN, Gallo LH, Ko J, **Cardenas G**, Nelson KN, Siari A, Campos AR, Whisenant TC, Donoghue DJ. Oncogenic Mutation in IKKβ function through global changes induced by K63-linked ubiquitination and result in autocrine stimulation. 2018.

VITA

2014	Bachelor of Science, University of California San Diego
2014-2017	Research Associate I and II at Sirenas LLC
2017-2018	Teaching Assistant, University of California San Diego
2018	Master of Science, University of California San Diego

PUBLICATIONS

Meyer AN, Gallo LH, Ko J, **Cardenas G**, Nelson KN, Siari A, Campos AR, Whisenant TC, Donoghue DJ. Oncogenic Mutation in IKKβ function through global changes induced by K63-linked ubiquitination and result in autocrine stimulation. PLOS one. 2018

FIELD OF STUDY

Major Field: Biochemistry

Studies in Biochemisty

Professor Daniel J. Donoghue

ABSTRACT OF THE THESIS

Investigating the Role of K63-linked Polyubiquitination in Oncogenic IKKβ and BRAF Mutants

by

Guillermo Cardenas

Master of Science in Chemistry

University of California San Diego, 2018

Professor Daniel J. Donoghue, Chair

Aberrant signaling from mutations at K171 in the kinase domain of IKKB is known to occur in multiple myeloma, spleen marginal zone lymphoma, and mantle cell lymphoma. Previous work demonstrated that constitutive kinase activation stimulates Signal Transducer and Activator of Transcription 3 (STAT3). Using mass spectrometry, we identified K147 as a site for K63-linked ubiquitination that only occurs in mutant IKKB K171E. The crosstalk between this IKKβ mutant and the Janus Kinases (JAKs) pathway was further investigated by using an IL-6-responsive cell line, which showed that IKKβ 171E mutants stimulates the release of IL-6 into conditioned media. This suggests that it triggers an autocrine loop in which IL-6 is secreted and binds to its own IL-6 receptor-gp130 complex, resulting in JAK activation. Lastly, proteins

associated with K63-only-ubiquitinated IKKβ K171E were examined using mass spectrometry, and using proteomic analysis, activation of proteins and pathways involved in proliferative responses were found. Knowing that cancers harboring the K171E mutation on IKKβ can also activate STAT3 along with p44/42 MAPK (Erk1/2), the possibility of using MAPK and JAK inhibitors, or specific ubiquitination inhibitors as treatments should be investigated.

Mutations found on Rapidly Accelerated Fibrosarcoma homolog B (B-raf) have been identified in about 50% of melanomas, 90% of which harbor the V600E point mutation [58]. One study has shown that the activating mutant V600E is regulated by K63-linked polyubiquitination at K578 [40]. Here we further examine the polyubiquitination on B-raf by creating a kinase dead mutation, K483R, and the identified ubiquitination site K578 mutated to arginine, both in V600E background. V600E was found to have increased polyubiquitination, however, K578R does not seem to be the only lysine responsible for polyubiquitination. When observing K63 linkage specificity, V600E polyubiquitination does not seem to be entirely K63-linked, therefore UBE2N was not seen to be the E2 responsible for the ubiquitination signal. The K483R mutation, or the kinase dead BRAF, was able to abolish P-MAPK signal but not polyubiquitination, meaning that the kinase is not required for polyubiquitination of itself. The K578R mutation was able to reduce the P-MAPK signal, but was not able to completely abolish the polyubiquitination signal, meaning that there are other lysines that may be polyubiquitinated.

1.1 Introduction

Ubiquitination is an enzymatic post-translational modification that occurs in eukaryotes which attaches a regulatory protein, ubiquitin, to a substrate protein to mark it for a variety of cellular functions such as degradation, localization, controlling protein-protein interactions, activating or inactivating proteins [1]. There are three types of enzymes that are required for this modification, a ubiquitin-activating enzyme (E1), a ubiquitin-conjugating enzyme (E2), and a ubiquitin ligase (E3) [2]. First, E1 binds both ATP and ubiquitin and adenylates the c-terminus (G76) on ubiquitin. Then, the ubiquitin-AMP intermediate is transferred to a cysteine on E1 with a thiol-ester bond forming with G76 on ubiquitin, releasing AMP [3]. E2 then binds to both E1 and activated ubiquitin and transfers the ubiquitin onto its own active cysteine via a transesterification reaction. An E3 then binds to a loaded E2 and a substrate and catalyzes an isopeptide bond between the lysine on a substrate and the c-terminus of a ubiquitin [3]. Currently, there have been 2 E1s, 50 E2s, and 600 E3s identified in humans [4], meaning specificity to substrates is limited to E2s and E3s.

Substrates can also be polyubiquitinated, meaning another ubiquitin proteins can be ligated onto the initial G76 linked ubiquitin by E2 and E3s again. Ubiquitin has seven ubiquitination sites: K6, K11, K27, K29, K33, K48, K63, and M1, and they can be re-arranged into several types of polyubiquitination, such as chained, branched, and even heterologous chains involving ubiquitin-like proteins [5]. K48 linkages have been well studied and have been known to signal a protein for proteasomal degradation, but of particular interest are K63 linked ubiquitination. K63 polyubiquitination is a non-degradative chain known for non-traditional functions such as DNA damage repair, protein trafficking, transcriptional regulation, and kinase signaling [6][7][8][9]. In cancers, K63 linked polyubiquitination can assist in a protein's stability and ultimately its evasion to degradation.

Inhibitor of nuclear factor kappa B, or IKKβ, is a subunit of IKK complex with a serine kinase activity. Being part of the nF-κB pathway, it can be activated by a variety of stimuli such as cytokines, bacterial or viral products, DNA damage, or cellular stress [10]. In the canonical pathway, proinflammatory cytokines, light-strand promoters, and growth factors like IL-1 and TNF activate their respective receptors, which subsequently activates the enzyme IkB kinase (IKK) [11]. Depending on the receptor, there are different downstream proteins involved such as TRAF or Tak1 that ultimately activates an IKK complex. An active IKK then phosphorylates the serine residues of the inhibitor of nF-KB (known as IkBα) which targets it for K48-linked polyubiquination and degradation by proteasomes. The free nF-kB then translocates into the nucleus and activates genes responsible for immune response, growth control, or apoptotic evasion [11]. Mutations in IKKB have also been implicated in survival, stemness, migration, and proliferation of many cancers including prostate cancer [12] and diffuse large B-cell lymphoma [13]. More specifically, mutations at position Lys171 in the kinase domain of IKKB have been identified in cancers such as multiple myeloma [14], splenic marginal zone lymphoma [15], and mantle cell lymphoma [16]. It has been demonstrated that mutations on Lys171 constitutively activates the protein intracellularly, without the need for extracellular signaling factors, and activates the Signal Transducer and activator of Transcription 3 (STAT3) pathway [17]. Previous work had also identified Lys147 as a site of K63-linked polyubiquitination, which is required for activation of the NF-kB pathway [17].

In the Janus Kinases (JAKs) pathway, the growth factor IL-6 binds to the IL-6 receptor (IL-6R), which causes it to dimerize with another receptor. IL-6 Signal Transducer (IL-6ST), also known as glycoprotein 130 (GP130), is a receptor subunit of the type I cytokine receptor and upon dimerization, the membrane bound JAKs become close in proximity and phosphorylate each other on tyrosine residues, activating their kinase domains [18]. Then the JAKs phosphorylate Tyr705 of cytosolic STAT3, which then dimerize on their phospho-tyrosine and their SH2 binding domains, and then translocate into the nucleus to activate their target genes

[18]. Overactivation of the STAT3 pathway has been known to drive proliferation, invasiveness, survival, as well as suppressing antitumor immune responses, and developing inhibitors for this pathway has been challenging because of the highly homologous domain of STAT proteins [19][20]. Specificity and potency have been an issue with the current JAK/STAT3 inhibitors, and severe toxicities arise with these treatments because of the physiological roles that STAT3 plays in mitochondrial metabolism and in the immune system [19]. Targeting NF-kB is also challenging because this pathway is critical for cell survival, and there are many pathways and proteins that can activate NF-KB. There are over 700 inhibitors for NFKB, however, many lack specificities and usually interfere with cellular inflammation, immune regulation, and cell homeostasis [21]. Therefore, looking for alternative targets that can be specific for an aberrant or overactivated pathway, such as kinases, phosphatases, and proteins involved in post-translational modifications are paramount.

Previous work from this lab speculates that a cross-talk exists between the IKK complex and the JAK pathway, therefore we pursued examining the pathways activated by the IKKβ mutants, as well as identifying protein interactions with the aberrant K63 polyubiquitination on oncogenic IKKβ K171E.

1.2 Results

1.2.1 Wild Type and mutant forms of IKKB

From previous work done by the lab, LC-MS/MS was used to show that IKKB is ubiquitinated at K147, K301, K418, K555, and K703, and that among those, only K147 was required for biological activity of the activated IKKB [17][22]. After removing these lysines, additional novel sites of ubiquitination were identified by LC-MS/MS analysis: K310, K428, K509, K614, and K641, and then removed to prevent ubiquitination at these sites and to isolate the effects of K147. Constructs were made with the original 4 identified lysines mutated to

arginines in WT, then another construct with all nine lysines mutated to arginines in WT (Figure 1.1A). Then the same constructs were made in the activating mutant K171E background (Figure 1.1B). Lastly, a construct was made on a highly conserved motif HRDLK[147] between the beta-6 and beta-7 domains of the N-terminal lobe of the kinase domain, K147R, known to significantly reduce the kinase activity (Figure 1.1C)[23][24].

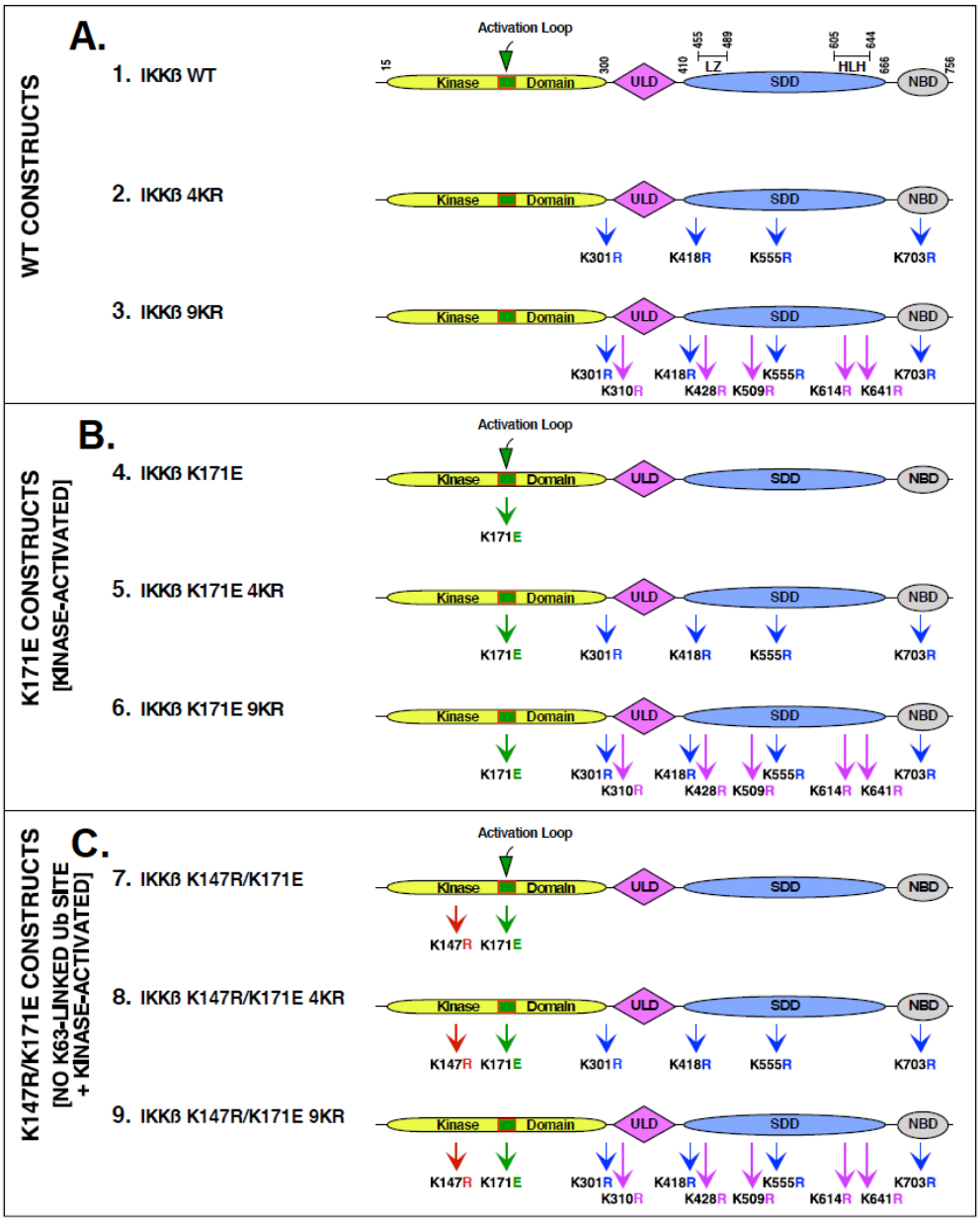

Figure 1.1 - IKKβ constructs. **A.** WT Constructs. Multiple sites of ubiquitination in IKKβ were identified by LC/MS-MS and then removed by site-directed mutagenesis. The IKKβ 4KR mutant was constructed with the mutations K301R, K418R, K555R, and K703R. Further analysis revealed additional ubiquitination sites, therefore five more lysines were removed in IKKβ 9KR; K310R, K428R, K509R, K614R, and K641R. **B.** K171E Constructs. The kinase activating mutation K171E was introduced into the constructs shown in (A) to create IKKβ K171E, IKKβ K171E 4KR, and IKKβ K171E 9KR. **C.** K147R/K171E Constructs. The mutation K147R, identified as a major site of K63-linked ubiquitination and required for IKKβ kinase activity [17], was introduced into the constructs shown in (B) to create IKKβ K147R/K171E, IKKβ K147R/K171E 4KR, and IKKβ K147R/K171E 9KR. The ubiqutin-like domain (ULD), the scaffold/dimerization domain (SDD) which contains the leucine zipper (LZ) and helix-looop-helix (HLH) regions, and NEMO binding domain (NBD) are indicated.

1.2.2 Activity of Wild Type and Mutant forms of IKKB

From previous studies, the IKKB constructs were examined for activation by using an antiserum that detects phosphorylation of IKKβ within the activation loop (Figure 1.2A). As shown, the proteins IKKβ WT, IKKβ 4KR, and IKKβ 9KR all exhibit activation (Lanes 1, 2, 3), but introduction of the K171E mutation strongly increases activation as seen by the phospho-IKKβ immunoblot (Lanes 4, 5, 6). In contrast, introduction of the kinase-dead mutation, K147R, nearly abolishes the phospho-IKKβ signal (Lanes 7, 8, 9).

We have previously utilized the phosphorylation of the signal transducing protein STAT3 to measure downstream signaling by activated IKKβ [17]. As shown in Figure 2B, the IKKβ mutants with the activating mutation K171E all exhibited strong activation of STAT3 signaling on the phospho-STAT3 blot (Lanes 4, 5, 6), indicating a non-canonical crosstalk between MAPK and the JAKs pathway. In either the WT background (Lanes 1, 2, 3), or in background of the kinase-dead mutation K147R (Lanes 7, 8, 9), significant phospho-STAT3 was not observed. The immunoblot of STAT3 was also done to show even expression of the protein throughout the samples (Figure 2B). In figure 2C, HA tagged ubiquitin was co-transfected with IKKB mutants, and after immunoprecipitation of the HA-Ubiquitin, lysates were blotted for IKKB to visualize polyubiquitination. The higher molecular band smear indicates the multiple ubiquitination chain formed on the protein. Here, polyubiquitination is only seen in the activating mutants (Lanes 4, 5, 6), showing that K171E is responsible for polyubiquitination of IKKB, and that K147 is the site of polyubiquitination.

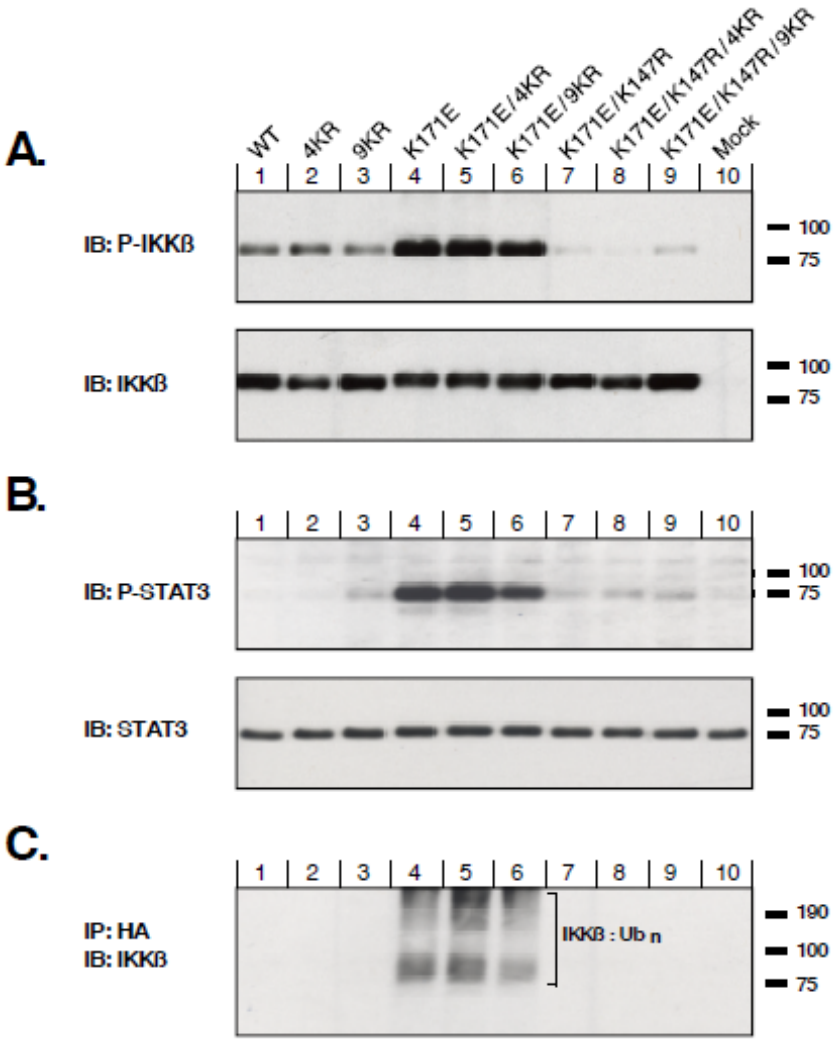

Figure 1.2 - Phosphorylation and ubiquitination of IKKβ. HEK293T cells were transfected with the IKKβ mutants together with HA-Ub3. Cells were lysed in RIPA and proteins separated by SDS-PAGE. **A.** Lysates were examined for activation of IKKβ kinase activity by immunoblotting for phospho-S177/S181 IKKβ. Total IKKβ expression is shown below. **B.** The same lysates as in (A) were examined for STAT3 signaling by immunoblotting for phospho-Y705-STAT3. Total STAT3 is shown below. **C.** HA-tagged ubiquitinated proteins from the same lysates were collected by immunoprecipitation, and HA-Ub-IKKβ was detected by immunoblotting for IKKβ.

1.2.3 Signaling Pathways activated by IKKB

The small-molecule inhibitor NSC697923 targets the E2 complex Ubc13-Uev1A and blocks the formation of K63-linked ubiquitin polymers that assists in activating the IKK complex during inflammation-induced activation of NFκB [25][26][27]. The effects of NSC697923 on activation of STAT3 is shown in Figure 1.3A (1st panel), in which the K171E constructs –

whether in the background of WT, 4KR, or 9KR – strongly activate phospho-STAT3 with the control vehicle DMSO (lanes 2-4). However, in the presence of NSC697923 the activation of phospho-STAT3 was reduced nearly to background levels (Lanes 6-8). Using an antiserum to detect phosphorylation within the activation loop of IKKβ (3rd panel), the inhibition of K63-linked ubiquitination by NSC697923 showed no inhibitory effect. Thus, K63-linked ubiquitination is required for the downstream activation of STAT3 by IKKβ, but not for activation of IKKβ itself.

IKKβ is typically activated by the upstream protein kinase TAK1 [28]. (5Z)-7-Oxozeaenol, a selective and irreversible inhibitor, covalently binds to TAK1 and abolishes downstream TAK1-induced MAPK signaling [29]. Cells expressing IKKβ WT together with TAK1/TAB exhibited phosphorylated STAT3 similar to the overexpression of IKKβ K171E alone, or to the results from IKKβ K171E co-expressed with TAK1/TAB (Figure 1.3B, 1st panel, Lanes 3-5). However, when treated with (5Z)-7-Oxozeaenol, STAT3 activation was reduced in these samples (Figure 1.3B, 1st panel, Lanes 8-10). Inhibition of TAK1 activity also abolished p44/42 MAPK (Erk1/2) signaling in cells expressing IKKβ K171E alone, or in cells expressing IKKβ constructs together with TAK1/TAB (Figure 1.3B, 3rd panel, compare Lanes 3-5 with 8-10). Notably, when co-expressed with TAK1/TAB, the phosphorylation of IKKβ WT was inhibited by the TAK1 inhibitor (Figure 1.3B, 5th panel, Lane 4 vs. 9), whereas phosphorylation of IKKβ K171E was not (Figure 1.3B, 5th panel, Lane 5 vs 10). These results demonstrate a requirement for TAK1 in the downstream activation of STA3 in response to activated IKKβ.

STAT3 is typically activated via IL-6-induced dimerization of the gp130 subunits of IL-6R, subsequently activating the JAKs to phosphorylate STAT3 [30]. In order to examine the requirement for JAK kinases, the K171E mutants – in the background of WT, 4KR, or 9KR – were examined in the absence or presence of JAK Inhibitor I, which is an early inhibitor of JAK family members based on a benzimidazole core. Figure 1.3C (1st panel) shows the resulting inhibition of STAT3 phosphorylation in the presence of JAK Inhibitor 1 (Lanes 3-5 vs Lanes 9-11). In this experiment, we also showed that JAK Inhibitor 1 inhibited phosphorylation of STAT3

in response to exogenous IL-6 (Lane 13 vs 14). We also considered whether an autocrine signaling response to IL-6 was induced by IKKβ K171E mutants, therefore, an inhibitor to an IL-6 receptor was used to see if STAT3 activation required exogenous IL-6.

Figure 1.3D examines the requirement for the IL-6 signal transducer gp130, which is a transmembrane protein known to be a subunit for IL-6 receptor. Cells were starved and treated with the gp130 inhibitor SC144, after which they were incubated with conditioned media from HEK293T cells expressing the IKKβ K171E mutants. As seen (1st panel), conditioned media from cells expressing the K171E mutants – in the background of WT, 4KR, or 9KR – clearly stimulated phospho-STAT3, and this was completely blocked by the presence of the gp130 inhibitor SC144 (Lanes 3-5 vs Lanes 9-11). Again, as a control, SC144 completely inhibited the response to exogenously added IL-6 (Lane 13 vs 14). The data presented in Figure 1.3, Panels C and D, clearly demonstrate that the downstream effects of IKKβ K171E mutants require the activity of JAK proteins acting in concert with the IL-6 signal transducer gp130.

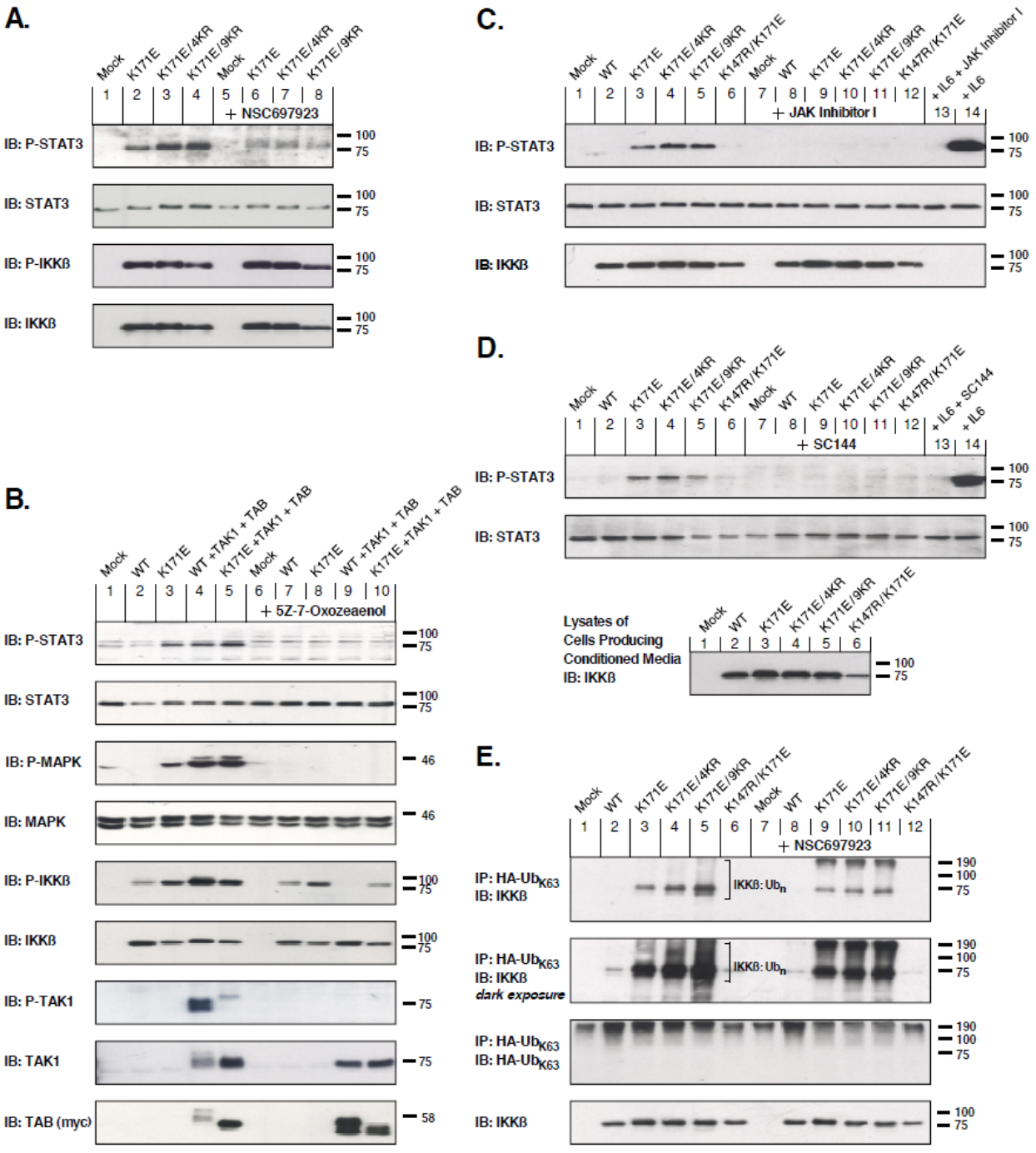

Figure 1.3 - Examination of STAT3 activation by activated mutants of IKKβ **A.** Requirement for K63-linked ubiquitination. HEK293T cells expressing IKKβ constructs were treated with NSC697923 (2μM for 2 hr) to inhibit UBE2N (Ubc13). STAT3 activation (1st panel) was detected by immunoblotting for phospho-Tyr705-STAT3, with total STAT3 shown below. The 3rd panel shows IKKβ kinase activation by immunoblotting for phospho-S177/S181 IKKβ, with total IKKβ shown below. **B.** Requirement for TAK1 activation. HEK293T cells expressing various combinations of IKKβ, TAK1 and TAB1 proteins were treated with 10 μM (5Z)-7- Oxozeaenol for 2 h to inhibit TAK1 activity. 1st Panel: STAT3 activation is shown by immunoblotting for phospho-Tyr705-STAT3. Total STAT3 is shown below. 3rd Panel: MAPK

Figure 1.3 Continued - activation, shown by immunoblotting for phospho-T202/Y204-MAPK. Total MAPK is shown below. 5th Panel: IKKβ kinase activation is shown by immunoblotting for phosphoS177/S181 IKKβ, with total IKKβ shown below. Panels 7-9: Controls are presented for TAB and TAK1 expression and activation using phospho-T184/187-TAK1, total TAK1, and myc (9E10) to detect myc-tagged TAB. **C.** Requirement for JAK activity. HEK293T cells expressing IKKβ mutants were treated with the Janus kinase inhibitor JAK Inhibitor 1 (2 μM for 2 hr). STAT3 activation is shown (top panel) by immunoblotting for phosphoTyr705-STAT3 **D.** Requirement for GP130. A requirement for gp130 function, which serves as the β subunit of the IL-6-Receptor, was examined using the gp130 inhibitor SC144. HEK293T cells were starved and treated with SC144 (25 μM for ~20 h) prior to a 2 h treatment with conditioned media from HEK293T cells expressing IKKβ mutants. STAT3 activation is shown (top panel) by immunoblotting for phospho-Tyr705-STAT3. Lysates from cells expressing the IKKβ mutants that generated the conditioned media is shown (3rd panel) after immunoblotting for total IKKβ. **E.** Specific increase of K63-Ubiquitin-IKKβ by activated IKKβ mutants. HEK293T cells expressing IKKβ mutants together with HA-tagged K63-only-Ubiquitin were treated with UBE2N inhibitor NSC697923 (2μM for 2 hr). Lysates were immunoprecipitated with HA antiserum, and then immunblotted to detect total IKKβ. The higher MW bands of IKKβ indicate K63-conjugated Ub complexes.

1.2.4 Inhibition of K63-linked ubiquitination

To further examine the ubiquitination of the IKKβ K171E mutants, we exploited an HA-tagged ubiquitin clone in which all Lys residues except for K63 were removed by mutagenesis. When co-expressed with IKKβ K171E proteins, it should result in a highly enriched signal for K63-linked ubiquitination. The results of this experiment are shown in Figure 1.3E (1st and 2nd panels), in the absence or presence of NSC697923 to inhibit the E2 ubiquitin conjugating enzyme UBE2N, known to catalyze K63 linked polyubiquitination (Lanes 3-5 vs Lanes 9-11). Although NSC697923 largely inhibits ubiquitination of IKKβ in this assay, it does not eliminate it completely. In the darker exposure, there is a very strong signal of polyubiquitinated IKKβ, indicated by the brackets, which is attenuated in the presence of the UBE2N inhibitor. These results demonstrate that ubiquitination of IKKβ K171E mutants significantly undergo a K63-linked pathway, but not entirely. Of note is the massive ubiquitination of the IKKβ K171E mutants in comparison with IKKβ WT, which is almost devoid of a ubiquitination signal except in the dark exposure (Figure 1.3E, 2nd panel, Lane 2). The higher molecular band seen in the top panel of Figure 1.3E under inhibitor conditions is thought to be endogenous NF-kB essential modulator (NEMO), which does get polyubiquitinated.

1.2.5 Proliferation of IL-6-dependent INA-6 cells by IKKβ K171E mutants

We investigated the biological significance of the K171E mutation by exploiting the murine myeloid 32D cell line which depends on exogenous IL-3 for proliferation and viability [31], and the INA-6 cell line, which is dependent upon exogenous IL-6 for proliferation [32]. In experiments with 32D cells, 32D cells were maintained to stably express IKKβ WT, K171E and K171E 4KR, but we were unable to demonstrate significant proliferative responses (data not shown). Experiments with INA-6 cells, however, did provide more insight (Figure 1.4). First, we established a dose response curve to IL-6 (Figure 1.4, Panel A), showing a very sensitive proliferative response by INA-6 cells. Next, we collected conditioned media from HEK293T cells expressing IKKβ mutants which, as shown above (Figure 1.3, Panel D), were capable of stimulating phospho-STAT3 when applied to HEK293T cells. When the conditioned media samples were applied to INA-6 cells in the absence of IL-6, proliferation was observed in response to IKKβ K171E, K171E 4KR, and K171E 9KR, which were essentially indistinguishable from one another. In contrast, neither IKKβ WT, nor kinase-dead IKKβ K147R K171E, were able to stimulate a proliferative response in INA-6 cells above the background condition of no IL-6 (Figure 1.4, Panel B). Phospho-STAT3 stimulation was also examined in the INA-6 cells treated with conditioned media for 48 h (Figure 1.4, Panel C). Overall, the data in Figure 1.4 demonstrates a secretion of either IL-6 itself, or another related cytokine, capable of eliciting a proliferative response in the IL-6 dependent cell line INA-6, in response to the activated IKKβ K171E proteins, with similar response observed for IKKβ K171E, IKKβ K171E 4KR, and IKKβ K171E 9KR.

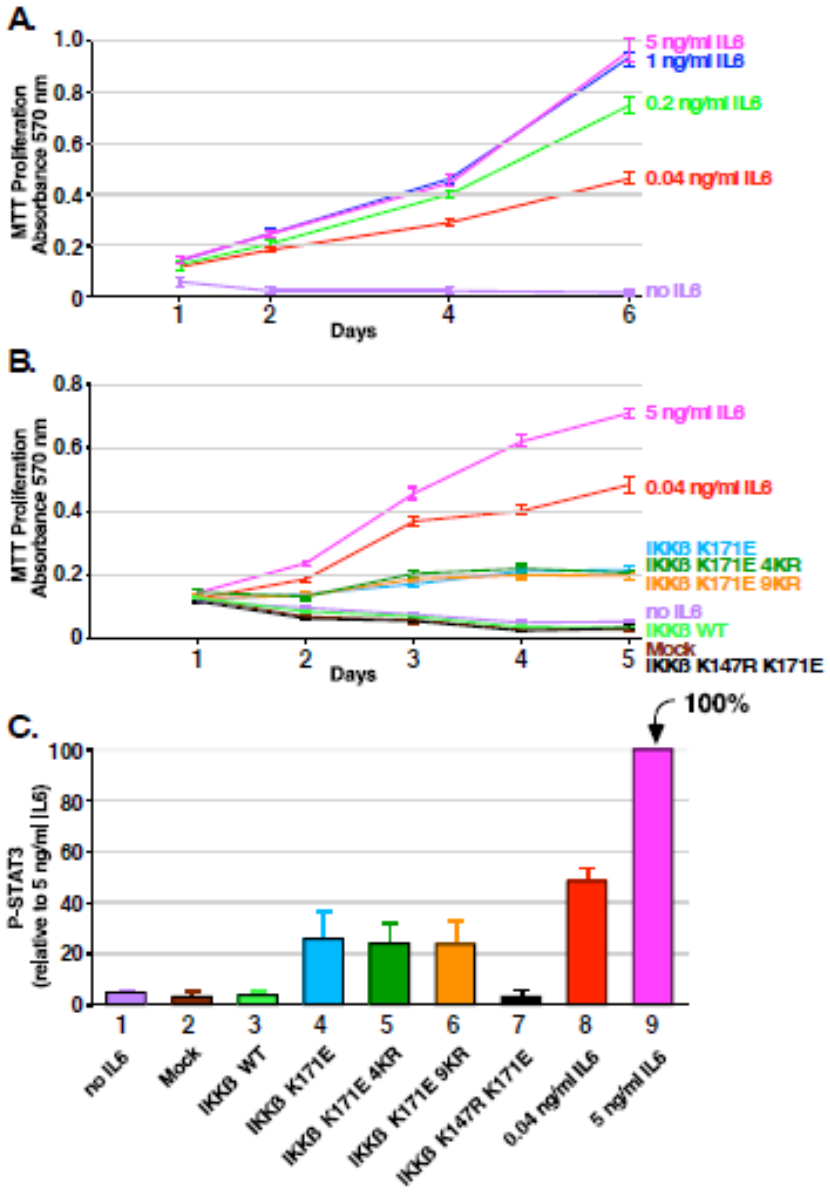

Figure 1.4 - Assessing the oncogenic potential of the K171E mutation in IKKβ on the IL-6 - dependent INA-6 cell line. The human myeloma cell line INA-6 is completely dependent on exogenous IL-6 for growth and proliferation. A. IL-6 concentration dependence of the INA-6 cells. Triplicate cultures of cells were grown in RPMI 1640 with 10% FBS and various concentrations of IL-6 (5, 1, 0.2, 0.04 and 0 ng/ml). Duplicate samples were collected at 1, 2, 4 and 6 days and assayed by MTT metabolic assay indicating the number of viable cells. Error bars show the standard deviation B. Proliferation of INA-6 cells treated with conditioned media. Triplicate cultures of INA-6 cells were incubated in media collected from HEK293T cells expressing IKKβ derivatives. 10% FBS was added to the starvation media. Duplicate samples were collected at 1, 2, 3, 4 and 5 days and assayed by MTT metabolic assay. Control samples were treated 5, 0.04 and 0 ng/ml of IL-6 as indicated. Error bars show the standard deviation C. STAT3 activation induced by conditioned media from cells expressing IKKβ mutants. INA-6 cells were incubated as in B. for 48 h. Cells were lysed and immunoblotted for P-STAT3. Triplicate immunoblots were quantitated with 5 ng/ml of IL-6 set at 100%. Error bars show the standard deviation.

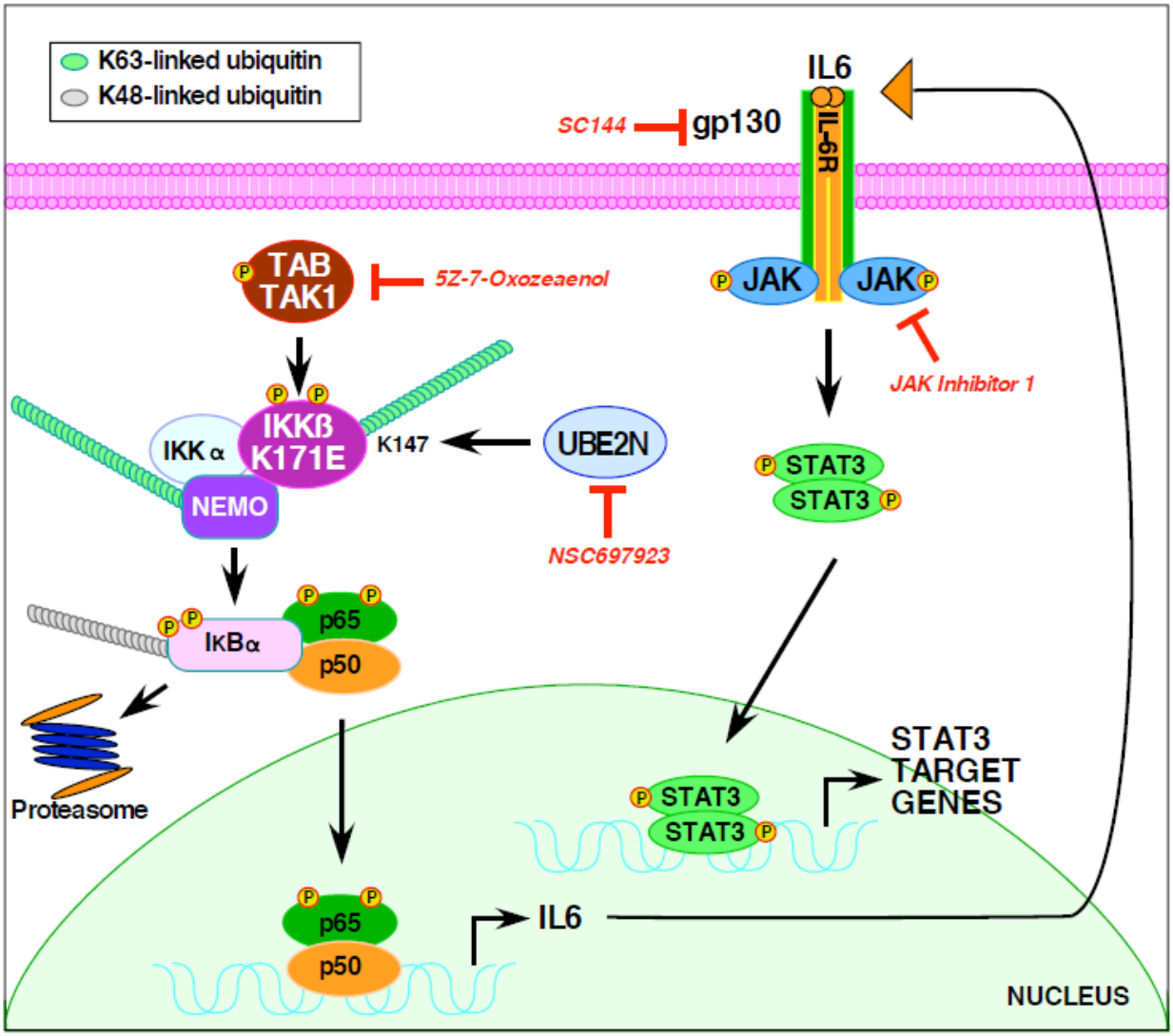

Figure 1.5 - Signaling Pathways Activated by K171E IKKβ. A model is presented for signaling by the oncogenic mutation K171E of IKKβ, identified in hematological malignancies, which integrates the data presented here. Normally, inflammatory cytokines activate NFkB and signal the K63-linked ubiquitination of TAK1 and NEMO, leading to the activation of the IKK complex and NFkB nuclear translocation. The K171E mutation of IKKβ instead leads to the K63-linked ubiquitination of K147 by UBE2N (Ubc13), as shown by the inhibitor NSC697923, and this activation is dependent upon the activity of TAK1, as shown by the inhibitor 5Z-7-Oxozeaenol. The IKKβ K171E mutants establish an autocrine loop dependent upon the secretion of IL-6, binding to the IL-6 receptor, as shown by the inhibitor SC144 which inhibits the β-subunit gp130. The involvement of the JAK kinase family (JAK1, JAK2, JAK3, TYK2) in this system is shown by 33 the inhibitor JAK Inhibitor 1, which also inhibits the appearance of phospho-STAT3 in response to IKKβ K171E mutants.

1.2.6 Molecular functions activated by IKKβ K171E mutants

To probe the changes in the abundancy of total proteins and of ubiquitin-conjugated proteins as a result of activated IKKβ K171E mutants, we employed a proteomics approach.

Large samples of 1.8x10e7 HEK293T cells were prepared co-expressing IKKβ WT or IKKβ K171E 9KR with HA-tagged K63-only-Ub. Four replicates of each sample were prepared. These lysates were immunoprecipitated with anti-HA mAB, subjected without further purification or enrichment by LC-MS/MS, and spectral data was then analyzed by MaxQuant label free quantitation (LFQ) [33]. This approach depended upon the hypothesis that the population of detectable proteins in these two groups would be different, as measured by the amounts and identities of the proteins. We wished to determine what pathways and functions are enriched in each group. As presented in Figure 1.6A, MaxQuant LFQ protein data [33] containing 3,237 initial proteins were analyzed using the Perseus Software/R environment [34][35] and, after removal of low abundancy and Crapome proteins [36], 958 proteins remained. Using a Student's T-test and false discovery threshold of 0.1, 265 proteins were identified as significantly differentially abundant between the IKKβ WT and IKKβ K171E 9KR groups. The major Gene Ontology, KEGG, and Panther categories identified after performing an enrichment analysis on these protein groups are presented in Figure 1.6B and are primarily related to ubiquitin ligases, ubiquitin-like protein transferases and binding, and ubiquitin proteasomal degradation pathways.

Analysis also revealed significant association with several E2 components, including UBE2N but also several others, as well as several HECT type E3 ligases. A partial summary of these data is presented in Figure 1.6C. Analysis by Gene 12 Set Enrichment Analysis (GSEA) [37][38], yielded several particularly interesting gene sets, two of which are presented here: Figure 1.6D presents proteins identified in KEGG UBIQUITINATED MEDIATED PROTELYSIS that were positively correlated with IKKβ WT samples (i.e. increased abundance relative to IKKβ K171E 9KR); and Figure 1.6E presents proteins identified in REACTOME G1 S TRANSITION that were negatively correlated with IKKβ WT samples (i.e. decreased abundance relative to IKKβ K171E 9KR). These proteins, indicating a role in progression through G1/S of the cell

cycle, are consistent with the overall proliferative responses described previously for activating IKKβ K171E mutants.

Figure 1.6 - Network Analysis in Response to Activated Mutants of IKKβ. **A.** Proteomic Analysis Pipeline. Schematic representation of the analysis steps for proteomic mass spectrometry data that uses MaxQuant Label Free Quantification values of detected proteins as input and generates a list of significantly differentially abundant proteins (Benjamini-Hochberg adjusted p-value < 0.05) as output. **B.** Top Biological Categories in Proteomic Analysis. Gene Ontology, KEGG, Panther, and Reactome pathways/categories identified as significantly enriched by WebGestalt (FDR < 0.05) for the list of differentially abundant proteins identified in (A). **C.** Pathway Level Representation of Select Differentially Abundant Proteins. Representative sub-processes of the significantly enriched Ubiquitin Mediated Proteolysis KEGG category from (B) that have a high percentage overlap with the differentially abundant protein list. Red boxes indicate proteins with significantly different abundance between the IKKβ WT and IKKβ K171E 9KR sample groups. **D.** Top GSEA Result for IKKβ WT. Using the list of 958 proteins identified in the two groups as input, the GSEA identified Gene set (KEGG Ubiquitin Mediated Proteolysis) with the highest Enrichment Score (ES) in IKKβ WT along with a heatmap of the top genes contributing to the ES. **E.** Top GSEA Result for IKKβ K171E 9KR. As in (D), the Gene set (Reactome G1 to S Transition) with the highest ES in IKKβ K171E 9KR along with the corresponding heatmap. In the heatmaps, the range of colors (red, pink, light blue, dark blue) shows the range of expression values for each gene in each sample (high, moderate, low, lowest).

A.

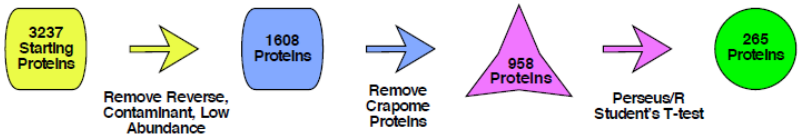

B.

Ontology	ID	Category
GO Molecular Function	GO:0019787	UBL protein transferase activity
GO Molecular Function	GO:0031072	Heat shock protein binding
GO Molecular Function	GO:0044389	UBL protein ligase binding
GO Molecular Function	GO:0032182	UBL protein binding
KEGG	hsa04120	Ub mediated proteolysis
Panther	P00060	Ub proteasome pathway
Reactome	R-HSA-8866652	Roles of E1 and E2 enzymes
Reactome	R-HSA-8852135	Protein ubiquitination

C.

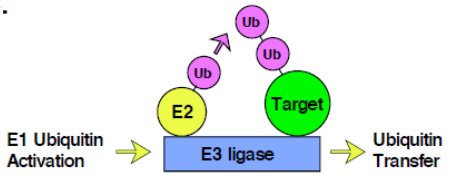

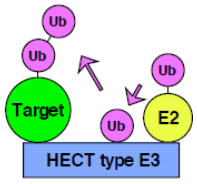

E2 Ubiquitin-conjugating enzymes

UBE2A	UBE2B	UBE2C	UBE2D	UBE2E
UBE2F	UBE2G1	UBE2G2	UBE2H	UBE2I
UBEJ1	UBEJ2	UBE2L3	UBE2L6	UBE2M
UBE2N	UBE2O	UBE2Q	UBE2R	UBE2S
UBE2U	UBE2W	UBE2Z	HIP2	BIRC6

HECT type E3 ubiquitin ligases

E6AP	UBE3B	UBE3C
Smurf	Itch	WWP1
WWP2	TRIP12	NEDD4
ARF-BP1	EDD1	HERC1
HERC2	HERC3	HERC4

D.

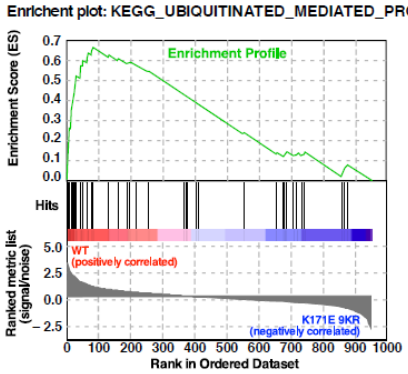

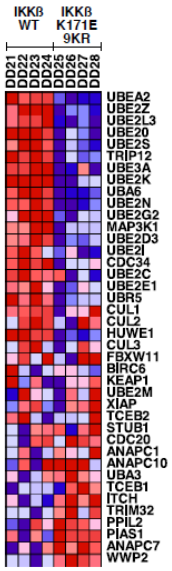

E.

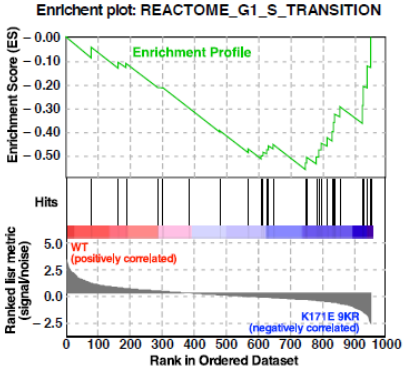

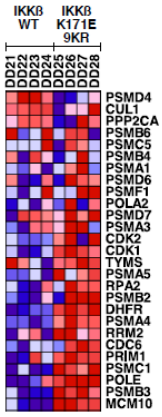

1.3 DISCUSSION

These experiments helped probe the signaling pathways activated by the oncogenic K171E mutation of IKKβ, originally identified in hematological malignancies [14][15][16]. The K63-linked ubiquitination of K147 is upregulated by the K171E mutation, which induces activation of STAT3. Throughout, we have focused our efforts on detecting Tyr705 phosphorylation of STAT3 in response to K171E mutations in IKKβ, since cytokine-mediated activation of phosphorylation at this site has been extensively shown to lead to nuclear translocation of STAT3. Initially, we had hoped we might create an IKKβ K171E mutant in which the only remaining site of ubiquitination would be K147. However, after eliminating more and more lysines, different lysines were then observed to be highly modified with ubiquitin. Therefore, rather than eliminating all other lysine sites, just enough were until K147 was preferentially ubiquitinated. First, the sites initially identified as ubiquitination sites, K301, K418, K555, and K703, were mutated to arginine to create the 4KR mutants. Although this resulted in a slight relative increase in utilization of K147 for ubiquitination, many additional sites of ubiquitination were now observed. We then eliminated K310, K428, K509, K614, and K641 along with the 4KR mutants to create the 9KR mutants. Although K147 was now preferentially utilized, we still saw the appearance of many ubiquitination sites. We found few changes in the ability of these different mutants to activate downstream pathways; as discussed below, IKKβ K171E, IKKβ K171E 4KR, and IKKβ K171E 9KR all exhibited relatively similar activation of downstream pathways. K63-linked ubiquitination in IKKβ, TAK1 and BRAF K63-linked ubiquitination stabilizes signaling functions of proteins and is an indispensable modification for the activation of innate and acquired immune responses, including DNA damage repair pathways [39].

Activation of the IKK complex and canonical NFκB signaling depends upon K63-linked ubiquitination of TAK1 and the linear ubiquitination of NEMO [22][23]. We show that the

activating mutation K171E of IKKβ upregulates K63-linked ubiquitination at K147, an evolutionarily conserved residue that modulates the kinase function of IKKβ [17]. K63- linked ubiquitination has also been reported in other noteworthy kinases at sites homologous to the K147 site in IKKβ. One example is K63-linked ubiquitination at K158 in TAK1, required for NFκB signaling during inflammatory responses [24][25][26]. Another example is K63-linked ubiquitination at K578 in BRAF V600E [40], which serves as an oncogenic driver in melanoma, lung and colorectal cancer [41]. Therefore, while the outcome of K63-linked ubiquitination at these sites may differ from that described here for IKKβ, it is significant that multiple kinases undergo regulatory K63-linked ubiquitination at this homologous residue to modulate inflammation and oncogenicity. A model integrating our results in presented in Figure 1.5. First, the K63-linked ubiquitination of IKKβ is required for activation of STAT3, as shown by the use of the inhibitor NSC697923 [40]. This result is consistent with our earlier work [17]. Surprisingly, although TAK1 activity was not required for activation of K171E kinase activity, as indicated by S177/S181 phosphorylation of the IKKβ activation loop, TAK1 activity was required to observe the subsequent activation of STAT3. This was revealed through the use of the TAK1 inhibitor (5Z)-7-Oxozeaenol [41][42]. Clearly, the IKKβ K171E mutants activate an autocrine loop in which IL-6 is secreted and subsequently binds to the IL-6 receptor complex gp130, resulting in JAK activation. This was shown using the gp130 inhibitor SC144 [43][44] and using the JAK/TYK2 inhibitor JAK Inhibitor 1 [45][46][47], both of which inhibited the appearance of phospho-STAT3 in response to IKKβ K171E mutants. The release of either IL-6 or a closely related molecule was directly demonstrated by collecting conditioned media from HEK293T cells expressing the IKKβ K171E mutants and showing: 1) these conditioned media resulted in STAT3 activation when applied to naive cells; and 2) these conditioned media stimulated proliferation and STAT3 activation of the IL-6-dependent cell line INA-6 [32] in the absence of exogenous IL-6. We also employed a proteomics approach to compare cells expressing IKKβ WT in comparison with IKKβ K171E 9KR, examining all proteins recovered that were labeled

with a co-expressed HA-tagged K63-only-Ub. These proteins were analyzed without further purification or enrichment by LC-MS/MS and MaxQuant label free quantitation [33]. We found that the populations of detectable proteins in these two groups were different as measured by the amounts and identities of the proteins. The major Gene Ontology, KEGG, and Panther categories identified were primarily related to ubiquitin ligases, ubiquitin-like protein transferases and binding, and ubiquitin proteasomal degradation pathways. Significant association was revealed with several E2 components, including UBE2N but also several others, as well as several HECT type E3 ligases. Among a number of different gene sets identified, proteins involved in ubiquitinated mediated proteolysis had abundance increased in the IKKβ WT sample group, whereas proteins associated with cell cycle progression had abundance increased in the IKKβ K171E 9KR sample group. These analyses reveal a major disruption of cellular ubiquitination functions by the activating mutation K171E, and reinforce the other experiments presented here that demonstrate an IL-6-independent proliferative advantage conferred by IKKβ K171E. This is also consistent with the activation of phospho-STAT3, shown throughout this work, which plays a major role as a transcriptional activator for many genes including those involved in the regulation of cell proliferation [48].

Identification and construction of IKKB mutants was done by Leo Gallo and Juyeon Ko. Western blot analysis were performed by April Meyer, Leo H. Gallo, Juyeon Ko and Guillermo Cardenas*. IL-6 experiments and mass spectrometry samples were prepared and ran by Alex Campos through an LC/MS/MS mass spectrometer at Sandford Burnham Prebys. Proteomics data was analyzed and put together by Thomas C. Whisenant from the Center for Computational Biology and Bioinformatics at UCSD.

1.4 Conclusion

From this work, we conclude that IKKB K171E is responsible for the K63 polyubiquitination of K147, and that this polyubiquitination is required for STAT3 activation, but not for IKKB phosphorylation. UBE2N (or Ubc13) was found to be the E2 responsible for the K63 linkage on K147 based off the inhibitor western blots. TAK1 was found to be required for STAT3 activation in the activating mutant K171E, and that this mutant undergoes an aberrant signaling pathway in where an autocrine loop is stimulated to activate the JAKs pathway. Lastly, using proteomic analysis, proteins associated with IKKβ K171E pathway were found to be involved in proliferative responses, more specifically those involved in the G1/S transition phase. This phase marks a point of no return, in where the cell decides to begin DNA replication and ultimately division, becoming unresponsive mitogenic factors.

The identification of IKKβ mutations at position 171 in hematological malignancies [14][15][16] suggests that their oncogenic potential depends on a specific cellular phenotype and genetic program. Patients with multiple myeloma, for instance, are usually treated with Bortezomib, a proteasome inhibitor that attenuates aberrant NFκB signaling. However, Bortezomib resistance is inevitable [49], demonstrating that Bortezomib-mediated inhibition of NFκB signaling may not be sufficient to achieve successful treatment. Cancers harboring K171-mutated IKKβ are likely to also exhibit activated STAT3 and p44/42 MAPK (Erk1/2), suggesting the possibility of using MAPK (Erk1/2) and JAK inhibitors, or specific ubiquitination inhibitors.

1.5 Materials and Methods

Plasmid constructs

IKKB constructs were made from previous members of the lab. Starting with expression plasmids for IKKβ WT and IKKβ K171E [17], IKKβ WT 4KR (K301R, K418R, K555R and K703R) and IKKβ K171E 4KR were generated by QuikChange site-directed mutagenesis

(Agilent). These constructs were then used for further mutagenesis to create the IKKβ WT 9KR (K301R, K310R, K418R, K428R, K509R, K555R, K614R, K641R, K703R) and IKKβ K171E 9KR plasmids (paper Figure 1). Kinase-dead derivatives were made by introduction of the K147R mutation. hTAK1 in pCMV6-XL5 was a gift from Dr. Leslie Thompson (UC Irvine) and myc-TAB1 in pcDNA3 was a gift from Dr. Carol Prives (Columbia University). The HA-Ub3 and HA-Nemo plasmids were described previously [17]. The HA-K63-only-Ub (K6R, K11R, K27R, K29R, K33R, K48R) plasmid was also generated by QuikChange site-directed mutagenisis (Agilent) in a pcDNA3 background; two rounds of mutagenesis were conducted, introducing the additional mutations together with new silent restriction sites, AgeI and NruI. The HA-K63-only Ub (K6E, K11E, K27E, K29E, K33E, and K48E) was also made in a similar fashion. The initial HA-Ub-K48R plasmid [50] was a gift from Cam Patterson (University of Arkansas), obtained from Andrea Carrano (UC SanDiego). All constructs were confirmed using DNA sequencing through Retrogen.

Cell Culture and INA-6 viability assay

HEK293T were grown in DMEM with 10% FBS and 1% Pen/strep and maintained in 10% CO2 at 37°C. Cells were transfected with plasmid DNA using calcium phosphate precipitation at 3% CO_2. Approximately 18 h after transfection, cells were starved overnight before collecting in RIPA Lysis Buffer with the following inhibitors: 10 ng/ml Aprotinin, 1 mM PMSF, 1 mM Na3VO4, 20 mM β-glycerol-phosphate, and 5 mM N-ethyl-maleimide. The IL-6-dependent multiple myeloma INA-6 cell line [32] was a generous gift from Dr. Erming Tian (University of Arkansas) and grown in RPMI 1640 with 10% FBS, 10% Marrow Max Bone Medium (Gibco Life Technologies), 10 ng/ml hIL-6 (R&D Systems) and maintained in 5% CO_2 at 37°C. To determine the IL-6 concentration dependence, INA-6 cells were seeded at an initial density of 2.5 x 10^5 cells/ml in media lacking Marrow Max Bone Medium, containing the indicated concentrations of hIL-6. Samples of triplicate cultures were removed and examined by

MTT metabolic assay at each time point. For MTT metabolic assays, 500 µl of cultures were transferred in duplicate to a 24-well TC plate and incubated with 50 µl of 5 mg/mL of thiazolyl blue tetrazolium bromide (MTT) (Sigma) at 37°C in 5% CO2 for 4 h, after which 500 µl of 0.04 M HCl in isopropanol was added and incubated again for at least 30 min. Absorbance was measured at 570 nm. IKKβ induced proliferation of INA-6 cells was determined by treating the cells with starvation media (RPMI1640) from HEK293T cells expressing IKKβ mutants. INA-6 cells were seeded at 3 x 10^4 cells/ml. FBS was added to sterile filtered starvation media prior to treatment at a 10% final concentration. Samples of triplicate cultures were removed and examined by MTT metabolic assay at each time point. To determine STAT3 activation, INA-6 cells seeded at 1.4 x 10^5 cells/ml were lysed in RIPA after 48 h incubation with media from HEK293T cells expressing IKKβ plasmids, prepared as described above. Lysates were immunoblotted as described below. Triplicate immunoblots were quantitated.

Electrophoresis, Immunoblotting and additional reagents

Lysates were collected in RIPA lysis buffer containing inhibitors 10 ng/ml Aprotinin, 1 mM PMSF, 1 mM Na3VO4, 20 mM β-glycerol-phosphate, and 5 mM N-ethyl-maleimide, and proteins were separated by 10% or 12.5% SDS-PAGE followed by transfer to Immobilon-P membrane. For immunoprecipitations, 400 µg of total protein was incubated with αHA (F7) overnight and collected with Protein A Sepharose (Sigma) or Pierce Protein A/B Magnetic Beads (Thermo Fisher Scientific). Immunoblotting reagents were from the following sources: antibodies against IKKβ (H-4), IKKβ (G-8), HA-probe (F-7), STAT3 (C-20), Myc (9E10), and TAK1 (M-579) from Santa Cruz Biotechnology; Phospho-IKKα/β (Ser176/180) (16A6), PhosphoSTAT3 (Tyr705) (D3A7), and Phospho-TAK1 (T184/187) (4531S) from Cell Signaling Technology; anti-FLAG from Sigma; HRP anti-mouse, HRP anti-rabbit, and Enhanced Chemiluminescence (ECL) reagents from GE Healthcare. Other reagents included: NSC697923 from Santa Cruz Biotechnology; JAK Inhibitor 1 from Calbiochem; MG132 and (5Z)-7-

Oxozeaenol from Tocris Bioscience; SC144 from Sigma-Aldrich; recombinant human IL-6 from R&D Systems.

Mass spectrometry and Network Analysis

From previous work done in the lab, identification of the ubiquitination sites were done by transfecting HEK293T cells with the indicated IKKβ plasmids together with HA-Ub3 and HA-NEMO plasmids. Cells were starved overnight and treated with 10 μM MG132 for at least 48 h before collection. Lysates were collected in RIPA and analyzed as previously described [17]. For IKKβ K171E, data presented previously in Table 1 of [17]. For IKKβ K171E 4KR, and IKKβ K171E 9KR, lysates were prepared in Sonication Buffer and subjected to sonication as described [51]. Lysates were immunoprecipitated with anti-IKKβ (H-4), and collected using 19 Pierce Protein A/G Magnetic Beads prior to analysis by LC-MS/MS. For the comparative analysis of IKKβ WT and IKKβ K171E 9KR, quadruplicate sets of $1.8x10^7$ HEK293T cells were transfected, together with HA-K63-only-Ub. Lysates were sonicated, immunoprecipitated with anti-HA (F-7), and collected using Pierce Protein A/G Magnetic Beads. Dried samples were reconstituted with 2% acetonitrile, 0.1% formic acid and analyzed by LCMS/MS using a Proxeon EASY nanoLC system (Thermo Fisher Scientific) coupled to a QExactive Plus mass spectrometer (Thermo Fisher Scientific). Peptides were separated using an analytical C18 Acclaim PepMap column 0.075 x 500 mm, 2 μm particles (Thermo Fisher Scientific) in a 94-min linear gradient of 2-28% solvent B at a flow rate of 300 nL/min. The mass spectrometer was operated in positive data-dependent acquisition mode. MS1 spectra were measured with a resolution of 70,000, an AGC target of 1e6 and a mass range from 350 to 1700 m/z. Up to 12 MS2 spectra per duty cycle were triggered, fragmented by HCD, and acquired with a resolution of 17,500 and an AGC target of 5e4, an isolation window of 1.6 m/z and a normalized collision energy of 25. Dynamic exclusion was enabled with duration of 25 sec. LC-MS/MS spectra were analyzed using the quantitative proteomics software package MaxQuant which was used for

peak detection, scoring of peptides, protein identification and label free quantification [33][34]. The MaxQuant output of quantified values for each protein in each sample was used as input to the Perseus software package which was used to remove proteins identified as contaminants or from a database of reverse proteins, impute absent values, log transform, and perform a width adjustment normalization on the data [17]. An additional filtering step removed proteins identified as bound non-specifically during the affinity purification. This list was generated by a search of the Crapome database with the parameters: HEK293 (cell type), HA (affinity tag), and magnetic beads (affinity support) [36]. 20 To identify proteins with significantly different abundance between the two sample groups, a Student's T-test, within the Perseus software, was performed on all proteins. An adjustment of the p-values for multiple testing was made using the Benjamini-Hochberg method. To identify significantly enriched pathways and functions (FDR < 0.05), the list of differentially abundant proteins was used as input into the WebGestalt package within the R statistical computing environment [52][53]. Gene Set Enrichment Analysis was performed on the complete list of identified proteins using the default parameters [37].

Antibodies, Immunoprecipitation, and Immunoblot

Antibodies were obtained from the following sources: IKKγ (FL-419), IKKβ (H-4), IKKβ (G-8), β-tubulin (H-235), HA-probe (F-7), STAT3 (C-20), IκBα (C-21) from Santa Cruz Biotechnology; Phospho-IKKα/β (Ser176/180) (16A6), K63-linkage Specific Polyubiquitin (D7A11), K48-linkage Specific Polyubiquitin (D9D5), Phospho-STAT3 (Tyr705) (D3A7), Phospho-IκBα (Ser32/36) (5A5) from Cell Signaling Technology; horseradish peroxidase (HRP) anti-mouse, HPR anti-rabbit from GE Healthcare. Enhanced chemiluminence (ECL) reagents were from GE Healthcare. TNFα and MG132 were obtained from Bio-techne; recombinant human Interleukin-6 (IL-6) from Life Technologies; and NSC697923 from Santa Cruz Biotechnology.

Twenty-four hours prior to transfection, cells were plated at a density of $1x10^6$ cells onto 100mm plates. Cells were co-transfected with 6ug of plasmid DNA using a calcium phosphate transfection method at 3% CO_2 for 18 hours. Cells were then recovered at 10% CO_2 for 6 hours before starving with DMEM for 18 hours. Then, cells were collected and lysed with RIPA with the following concentrations: 10 ng/ml Aprotinin, 1 mM PMSF, 1 mM Na3VO4, 20 mM β-glycerol-phosphate, and 5 mM N-ethyl-maleimide. For Inhibitor experiments, 1mL of 1mM NSC was added to cells 2hrs prior to collecting, with DMSO as the vehicle for the positive controls.

Chapter 1, in full, has been submitted for publication as it may appear in PLOS one, Meyer AN, Gallo LH, Ko J, **Cardenas G**, Nelson KN, Siari A, Campos AR, Whisenant TC, Donoghue DJ. Oncogenic Mutation in IKKβ function through global changes induced by K63-linked ubiquitination and result in autocrine stimulation. 2018

2.1 Introduction

The MAPK pathway, also known as the extracellular signal-regulated kinase (ERK) pathway, has been an extensively studied pathway known to be involved in cellular division, survival, and proliferation [54]. It begins with an extracellular mitogen, like a growth factor, binding to a growth factor receptor. The receptor then dimerizes and auto-phosphorylate themselves at their cytoplasmic domain with their tyrosine kinases. This creates a docking site for proteins with an SH2 domain, such as growth factor receptor bound protein 2 (GRB2), which binds and forms a complex with the guanine nucleotide exchange factor-1, or son of sevenless homolog 1 (SOS1). SOS1 becomes activates once the complex binds to the receptor, it removes the GDP from a Rat Sarcoma (Ras) protein. Ras then recruits GTP and can begin the kinase cascade, phosphorylating the Rapidly Accelerating Fibroblast (Raf) kinase, which then phosphorylates mitogen-activated protein kinase kinase (MEK), which phosphorylates mitogen-

activated protein kinase (MAPK or ERK). MAPK can phosphorylate several transcription factors, such as MNK, RSK, and c-Myc to name a few. These factors are involved in cell division and proliferation, therefore overactivation of this pathway can lead to cancerous cells [55].

Rapidly Accelerated Fibrosarcoma (RAF) is a serine/threonine protein kinase that participates in the mitogen-activated protein kinase (MAPK) pathway. There are three isoforms of RAF, and although they all activate the MAPK pathway, B-Raf is known to have a higher basal kinase activity than its other family members [56][57]. All three isoforms have been found to have implications in cancer, but most notably are the point mutations found in B-Raf. It has been found that 50% of melanomas harbor an activating BRAF mutation, and among those mutations, over 90% are at codon V600 [58]. The most common mutation is the V600E mutation found on the activation segment in the kinase domain, which causes constitutive activation of the of the kinase, as well as insensitivity to negative feedback mechanisms [59][60]. Currently, there only a few BRAF inhibitors approved by the FDA, the first being Vemurafenib, a BRAF V600E inhibitor approved for late stage melanoma back in 2011. Dabrafenib was then approved as well for BRAF V600 mutants, but now is currently given to patients in combination with the MEK inhibitor Trametinib. Resistance usually occurs within 6 to 8 months of a BRAF inhibitor, therefore, MEK inhibitors such as Cobimetinib were approved for use in combination with BRAF inhibitors to slow down the progression of drug resistance mechanisms and to improve efficacy [61][62]. Still, combination treatments only delayed resistance for a couple months, from 6 to 10 months [61]. Currently, new efforts are going into adding a third element to treatment, PD-L1 blockades, but regardless of new strategies, the search for new biomarkers and a thorough investigation of the BRAF V600E pathway is of dire importance.

Ubiquitination in the B-raf has not been fully characterized, but lysine sites have been suspected to be polyubiquitinated in activating mutants. K578R and K483R mutations were shown to reduce MAPK activity in activating mutant V600E, however K483R is located within the ATP-binding pocket of B-raf [40], therefore whether polyubiquitination plays a role in the

aberrant signaling is still unknown. Here we investigate the requirements for MAPK activation concerning polyubiquitination sites and types of polyubiquitination, as well as investigating Ubc13 (also known as UBE2N) as a possible E2 responsible for polyubiquitination similar to IKKB.

2.2 Results

2.2.1 Homology between BRAF and IKKB kinase domains

Comparing the homology between IKKB and BRAF on a BLAST database (Figure 2.1), we see that the kinase domains are significantly related to one another, therefore we suspect that lysine K578 would behave similarly to that of K147 in the kinase domain of IKKB. This ubiquitination site has been reported to be polyubiquitinated before, and it is found within a non-critical site in kinase domain [40]. Constructs were made as shown in figure 2.2; wildtype BRAF, BRAF with a known kinase dead mutation K483R, and BRAF with the lysine thought to be responsible for the K63 polyubiquitination mutated, K578R. These three constructs were also made in background of the activating mutant V600E using site directed mutagenesis.

Score	Expect	Method	Identities	Positives	Gaps
76.3 bits(186)	2e-18	Compositional matrix adjust.	59/221(27%)	105/221(47%)	30/221(13%)

```
Braf   455  GQITVGQRIGSGSFGTVYKGKWHGD-----VAVKMLNVTAPTPQQLQAFKNEVGVLRKTR  509
            G   + +R+G+G FG V +  WH        +A+K        +P+  + +  E+ ++R+
IKKβ   13   GAWEMKERLGTGGFGNVIR--WHNQETGEQIAIKQCR-QELSPRNRERWCLEIQIMRRLT  69

Braf   510  HVNILLF---------MGYSTKPQLAIVTQWCEGSSLYHHLHIIETKFEMIK--LIDIAR  558
            H N++           +  +  P LA+  ++C+G  L  +L+  E    + +  ++ +
IKKβ   70   HPNVVAARDVPEGMQNLAPNDLPLLAM--EYCQGGDLRKYLNQFENCCGLREGAILTLLS  127

Braf   559  QTAQGMDYLHAKSIIHRDLKSNNIFLH---EDLTVKIGDFGLATVKSRWSGSHQFEQLSG  615
              A  + YLH   IIHRDLK  NI L    + L  KI D G A    + S    F    G
IKKβ   128  DIASALRYLHENRIIHRDLKPENIVLQQGEQRLIHKIIDLGYAKELDQGSLCTSF---VG  184

Braf   616  SILWMAPEVIRMQDKNPYSFQSDVYAFGIVLYELMTGQLPY  656
            ++ ++APE++  Q    Y+   D ++FG + +E +TG  P+
IKKβ   185  TLQYLAPELLEQQ---KYTVTVDYWSFGTLAFECITGFRPF  222
```

Figure 2.1 - Homology between BRAF and IKKB kinase domains. BLAST analysis preformed between known sequences of wildtype BRAF and IKKB. K578 from BRAF and K147 from IKKB align in this analysis.

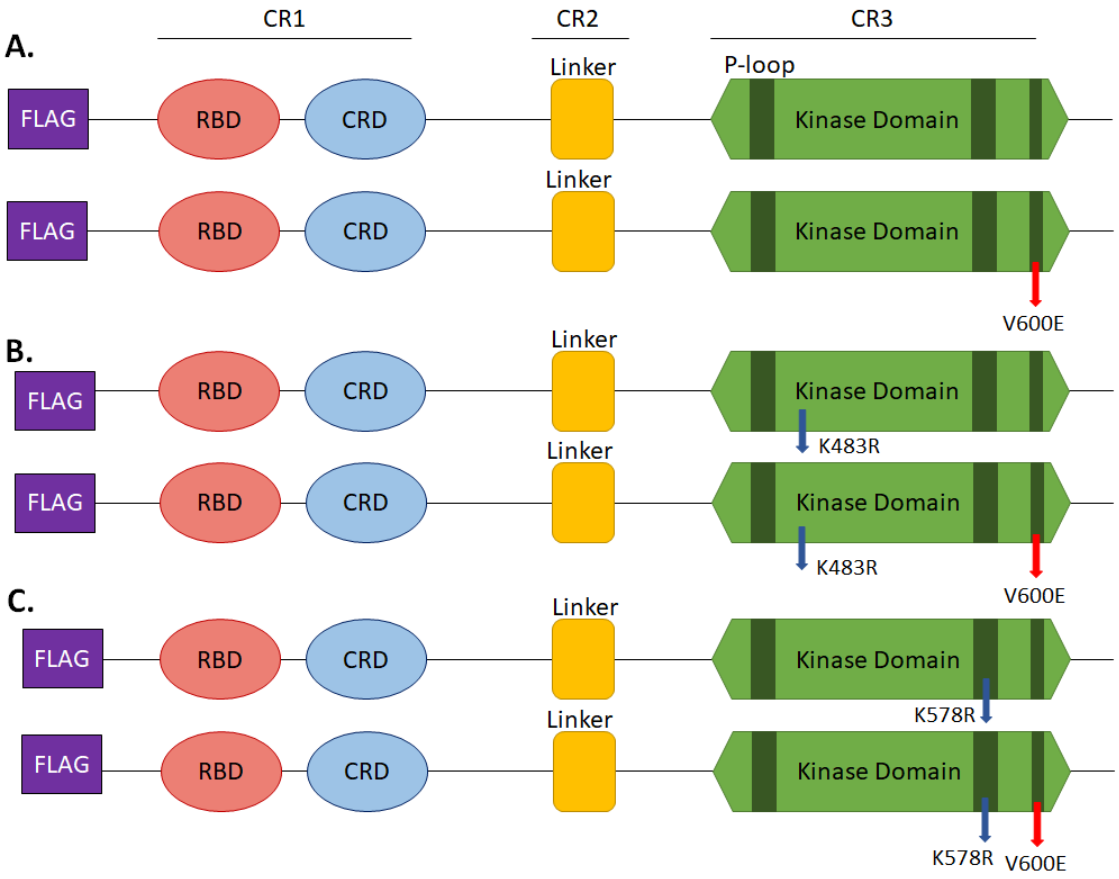

Figure 2.2 - BRAF V600E constructs. **A.** WT BRAF along with the activating mutant V600E. **B.** BRAF with the kinase dead mutation K483R in WT and V600E background. **C.** BRAF with the ubiquitination site K578R removed in WT and V600E background. Ras binding Domain (RBD) and cysteine rich domain (CRD) are shown as well.

2.2.2 Polyubiquitination of BRAF mutants

First, we investigated the polyubiquitination of the activating BRAF mutant along with its wildtype counterpart and the mutant K578R, shown to be a site for polyubiquitination (Figure 2.3). After co-expressing our K63-only Ubiquitin construct with the BRAF mutants, we pulled down on the HA-tagged Ubiquitin and blotted for the FLAG tag found on our expressed BRAF. The polyubiquitination observed should be K63 linked, but there may be endogenous polyubiquitination occurring. Endogenous BRAF should not be detectable. In Figure 2.3 we see polyubiquitination on the activating mutant and on the ubiquitination site removed, verifying that BRAF V600E is undergoing post-translational modification, and that the lysine site is not solely

responsible for polyubiquitination. In the presence of the NSC697923 inhibitor, a UBE2N inhibitor, polyubiquitination is not significantly reduced. The UBE2N-UBE2V1/2 complex has been known to elongate an already monoubiquitinated site with a K63-linkage, but if it is not responsible for the linkage seen then it points to the conclusion that there is another E2 responsible for the ubiquitination of activated BRAF.

Next, we introduced the kinase dead BRAF, along with the activating mutant in both kinase dead and with the lysine responsible for polyubiquitination removed (Figure 2.3). Panel A shows the FLAG tag blot of an Ha-Ubiquitin pull-down after co-transfecting cells with K63-only ubiquitin. Interestingly, polyubiquitination is seen on the V600E mutants regardless if it had the K483R or the K578R mutation. The K483R kinase dead mutant has ubiquitination, meaning that BRAF activity is not required for polyubiquitination. The polyubiquitination at the K578R mutation shows that K578 is not the only lysine site that gets polyubiquitinated, and perhaps may be behaving like IKKβ, where other lysines become polyubiquitinated after mutating away the dominant site. We then looked at the downstream signaling by blotting for phosphor-MAPK, along with lysate totals, and we see that mutants with the activation mutation V600E over activates the MAPK (or ERK1/2) pathway (Panel D). Mutants without the active mutation do not show over activation of the pathway and that polyubiquitination of BRAF at K578R is somewhat required for downstream P-MAPK signaling.

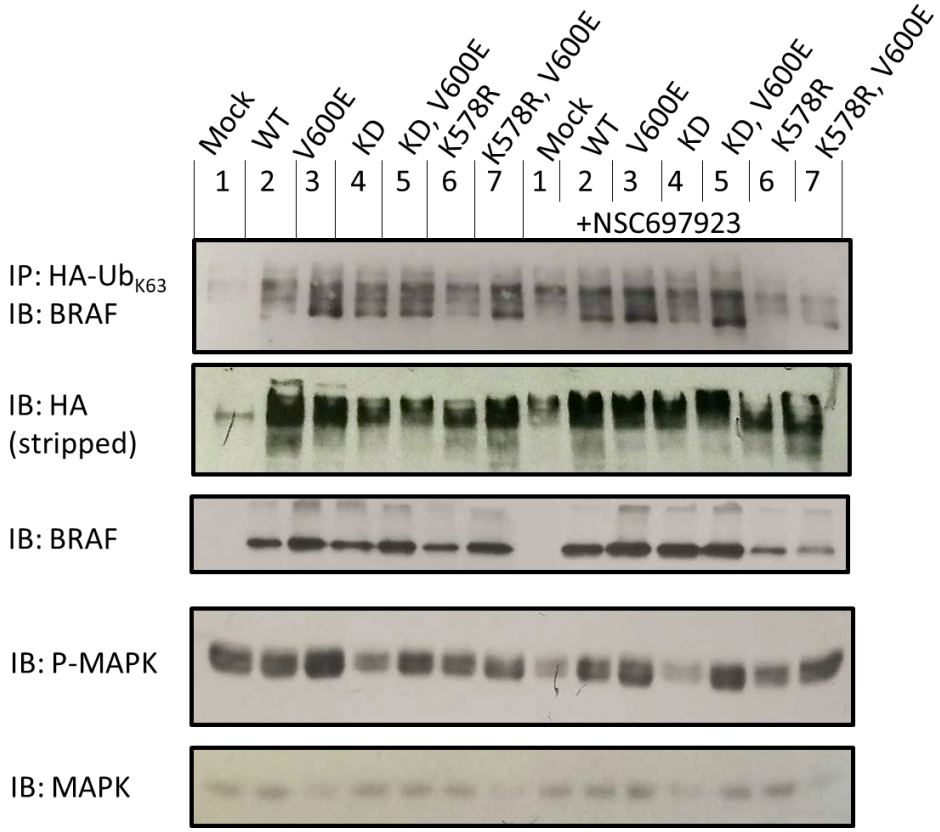

Figure 2.3 – Investigating BRAF kinase dead mutant K483R and BRAF ubiquitination site K578R in V600E background. Cells were co-transfected with K63-only Ub along with BRAF constructs, starved for 18 hrs, and collected. **A.** Shows an immunoprecipitation of Ha-Ub$_{K63}$, followed by an immunoblot for BRAF. **B.** Shows HA-Ub totals from the IP after stripping. **C.** Shows total BRAF from lysates. **D.** Shows P-MAPK for lysates. **E.** Shows MAPK totals for blots

2.2.3 BRAF Mutants with either unmodified or K63 only Ub

In Figure 2.4, we tried to determine whether the polyubiquitination signal observed could be seen by overexpressing Ha-UB$_3$, a plasmid with three regions encoding for ubiquitin, and again if we could observe any specificity between this unmodified ubiquitin and K63 linked ubiquitination. Comparing the wildtype versus the activating mutant in the first set (left side of Figure 2.4), we see that there is a significant increase in polyubiquitination, but when comparing the same two constructs in the K63 ubiquitin constructs we do not see much of an increase. This shows that the BRAF mutant does not increase K63-linked polyubiquitination, but it does increase some type of polyubiquitination. Furthermore, the phospho-MAPK blot (Figure 2.4,

Panel D) shows a decrease in signal with the K578R,V600E mutation versus V600E alone, showing that this ubiquitination site is involved in the aberrant MAPK overexpression.

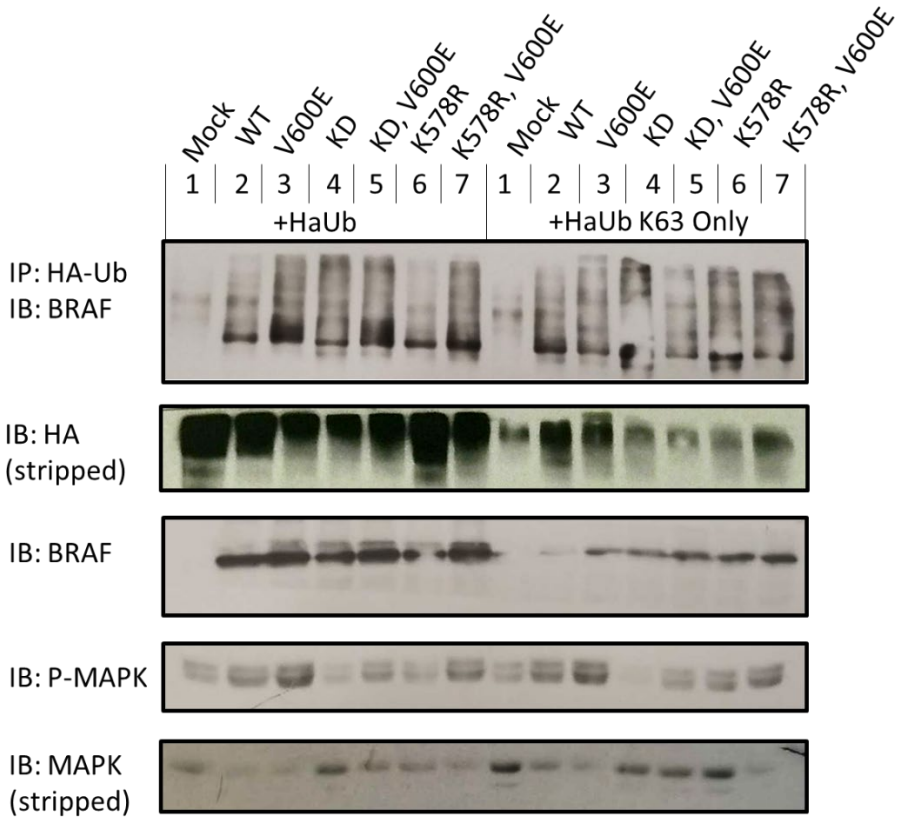

Figure 2.4 – Western Blot of BRAF mutants with either unmodified UB or K63 linked polyubiquitination. Co-transfections were done on HEK293T cells with BRAF mutants along with either K63 only HA-Ub or HA-UB unmodified. Cells were transfected, starved for 18hrs, and then collected. **A.** Shows an immunoprecipitation of Ha-Ub, followed by an immunoblot for BRAF. **B.** Shows HA totals for the IP after stripping. **C.** Shows BRAF totals for lysates. **D.** Shows phosphor-MAPK blot of lysates **E.** Shows MAPK totals from lysates after stripping.

2.3 Discussion

When looking at the effects of the activating mutant V600E, we still observe polyubiquitination regardless of kinase activity or the ubiquitination site K578R. The kinase must then not be required for polyubiquitination but is required for P-MAPK overexpression. The kinase dead construct has been shown to be the residue responsible for stabilizing the ATP in

the binding pocket [63], therefore any signal seen in the P-MAPK must be either a botting artifact or perhaps an imperfect transfection because it does seem to resemble the WT BRAF.

When observing at the phospho-MAPK signaling, there is over activation seen only for the V600E construct, but not for the other constructs. Overactivation of the V600E mutation does correlate with what is known in literature, and the K578 ubiquitination site does seem to be required for some downstream activation, even though it is not entirely K63 polyubiquitinated. We believe that a different type of chain is being formed in our activating V600E construct other than K63 linked or K48 linked. Those with a K48 linkage are likely to have been degraded, therefore another lysine linkage or branched chain is occurring in the V600E mutant. Wildtype BRAF may also be getting K63 polyubiquitinated for other pathways that are currently unknown, explaining why we see a signal for the wildtype construct and why it is difficult so see the difference in K63 linkages between itself and the activating mutant.

Previous reports have looked at polyubiquitination on all lysines found in the kinase domain [40], but polyubiquitination can occur at any structured domain [64]. There are many residues that would have to be investigated if we wanted to look at the source of the polyubiquitination signal, and a new approach may be needed. Running these samples through a mass spectrometer could help us identify new sites, and protein-protein interaction experiments such as an affinity column, an immunoprecipitation, or a BioID could provide us with more clues on the role of polyubiquitination.

2.4 Conclusion

From these experiments we gather that the non-canonical post-translational modification is occurring on BRAF V600E, and that K578 seems to be involved in P-MAPK overactivation in the activating mutant V600E. However, K578 is not an exclusive K63-polyubiquitination site.

UBE2N was therefore found to not be required for P-MAPK activation nor polyubiquitination at this lysine site.

Currently, there are a few inhibitors that have been approved for by the FDA such as Sorafenib and Vemurafenib, however tumors are sometimes unresponsive, and resistance occurs in many cases. Finding new and specific targets to tumors can have large impacts on current standards of treatment, therefore expanding the knowledge on BRAF and its polyubiquitination is of dire importance.

REFERENCES

1. Li, W., & Ye, Y. (2008). Polyubiquitin chains: functions, structures, and mechanisms. *Cellular and Molecular Life Sciences*, *65*(15), 2397-2406.

2. Hershko, A., & Ciechanover, A. (1998). The ubiquitin system.

3. Pickart, C. M. (2001). Mechanisms underlying ubiquitination. *Annual review of biochemistry*, *70*(1), 503-533.

4. Bhoj, V. G., & Chen, Z. J. (2009). Ubiquitylation in Innate and adaptive immunity. *Nature*, *458*(7237), 430.

5. Ikeda, F., & Dikic, I. (2008). Atypical ubiquitin chains: new molecular signals. *EMBO reports*, *9*(6), 536-542.

6. Messick, T. E., & Greenberg, R. A. (2009). The ubiquitin landscape at DNA double-strand breaks. *The Journal of cell biology*, *187*(3), 319-326.

7. Erpapazoglou, Z., Walker, O., & Haguenauer-Tsapis, R. (2014). Versatile roles of k63-linked ubiquitin chains in trafficking. *Cells*, *3*(4), 1027-1088.

8. Vallabhapurapu, S., & Karin, M. (2009). Regulation and function of NF-κB transcription factors in the immune system. *Annual review of immunology*, *27*, 693-733.

9. Wang, G., Gao, Y., Li, L., Jin, G., Chao, J. I., & Lin, H. K. (2012). K63-linked ubiquitination in kinase activation and cancer. *Frontiers in oncology*, *2*, 5.

10. Pahl, H. L. (1999). Activators and target genes of Rel/NF-κB transcription factors. *Oncogene*, *18*(49), 6853.

11. Demchenko, Y. N., & Kuehl, W. M. (2010). A critical role for the NFkB pathway in multiple myeloma. *Oncotarget*, *1*(1), 59.

12. Zhang Y, Lapidus RG, Liu P, Choi EY, Adediran S, Hussain A, Wang, X., Liu, X. and Dan, H.C. (2016). Targeting IκB kinase β/NF-κB signaling in human prostate cancer by a novel IκB kinase β inhibitor CmpdA. *Molecular cancer therapeutics*, molcanther-0999.

13. Agarwal, N. K., Kim, C. H., Kunkalla, K., Konno, H., Tjendra, Y., Kwon, D., Blonska, M., Kozloski, G.A., Moy, V.T., Verdun, R.E. & Barber, G. N. (2015). Active IKKβ promotes the stability of GLI1 oncogene in diffuse large B-cell lymphoma. *Blood*, blood-2015.

14. Chapman, M. A., Lawrence, M. S., Keats, J. J., Cibulskis, K., Sougnez, C., Schinzel, A. C., Harview, C.L., Brunet, J.P., Ahmann, G.J., Adli, M. & Anderson, K. C. (2011). Initial genome sequencing and analysis of multiple myeloma. *Nature*, *471*(7339), 467.

15. Rossi, D., Deaglio, S., Dominguez-Sola, D., Rasi, S., Vaisitti, T., Agostinelli, C., Spina, V., Bruscaggin, A., Monti, S., Cerri, M. and Cresta, S. (2011). Alteration of BIRC3 and multiple other NF-κB pathway genes in splenic marginal zone lymphoma. *Blood*, blood-2011.

16. Beà, S., Valdés-Mas, R., Navarro, A., Salaverria, I., Martín-Garcia, D., Jares, P., Giné, E., Pinyol, M., Royo, C., Nadeu, F. and Conde, L. (2013). Landscape of somatic mutations and clonal evolution in mantle cell lymphoma. *Proceedings of the National Academy of Sciences*, *110*(45), 18250-18255.

17. Gallo, L. H., Meyer, A. N., Motamedchaboki, K., Nelson, K. N., Haas, M., & Donoghue, D. J. (2014). Novel Lys63-linked ubiquitination of IKKβ induces STAT3 signaling. *Cell cycle*, *13*(24), 3964-3976.

18. Jatiani, S. S., Baker, S. J., Silverman, L. R., & Reddy, E. P. (2010). Jak/STAT pathways in cytokine signaling and myeloproliferative disorders: approaches for targeted therapies. *Genes & cancer*, *1*(10), 979-993.

19. Wong, A. L., Hirpara, J. L., Pervaiz, S., Eu, J. Q., Sethi, G., & Goh, B. C. (2017). Do STAT3 inhibitors have potential in the future for cancer therapy?.

20. Johnson, D. E., O'Keefe, R. A., & Grandis, J. R. (2018). Targeting the IL-6/JAK/STAT3 signalling axis in cancer. *Nature reviews. Clinical oncology*.

21. Gupta, S. C., Sundaram, C., Reuter, S., & Aggarwal, B. B. (2010). Inhibiting NF-κB activation by small molecules as a therapeutic strategy. *Biochimica et Biophysica Acta (BBA)-Gene Regulatory Mechanisms*, *1799*(10), 775-787.

22. Meyer, A. N., Drafahl, K. A., McAndrew, C. W., Gilda, J. E., Gallo, L. H., Haas, M., Brill, L.M. and Donoghue, D.J. (2013). Tyrosine phosphorylation allows integration of multiple signaling inputs by IKKβ. *PloS one*, *8*(12), e84497.

23. Xu, G., Lo, Y. C., Li, Q., Napolitano, G., Wu, X., Jiang, X., Dreano, M., Karin, M. and Wu, H. (2011). Crystal structure of inhibitor of κB kinase β. *Nature*, *472*(7343), 325.

24. Polley, S., Huang, D. B., Hauenstein, A. V., Fusco, A. J., Zhong, X., Vu, D., Schröfelbauer, B., Kim, Y., Hoffmann, A., Verma, I.M. and Ghosh, G. (2013). A structural basis for IκB kinase 2 activation via oligomerization-dependent trans auto-phosphorylation. *PLoS biology*, *11*(6), e1001581.

25. Hodge, C. D., Spyracopoulos, L., & Glover, J. M. (2016). Ubc13: the Lys63 ubiquitin chain building machine. *Oncotarget*, *7*(39), 64471.

26. Hodge, C. D., Edwards, R. A., Markin, C. J., McDonald, D., Pulvino, M., Huen, M. S., Zhao, J., Spyracopoulos, L., Hendzel, M.J. and Glover, J.M. (2015). Covalent inhibition of Ubc13 affects ubiquitin signaling and reveals active site elements important for targeting. *ACS chemical biology*, *10*(7), 1718-1728.

27. Pulvino, M., Liang, Y., Oleksyn, D., DeRan, M., Van Pelt, E., Shapiro, J., Sanz, I., Chen, L. and Zhao, J. (2012). Inhibition of proliferation and survival of diffuse large B-cell lymphoma cells by a small-molecule inhibitor of the ubiquitin-conjugating enzyme Ubc13-Uev1A. *Blood*, blood-2012.

28. Zhang, J., Clark, K., Lawrence, T., Peggie, M. W., & Cohen, P. (2014). An unexpected twist to the activation of IKKβ: TAK1 primes IKKβ for activation by autophosphorylation. *Biochemical Journal*, *461*(3), 531-537.

29. Wu, J., Powell, F., Larsen, N. A., Lai, Z., Byth, K. F., Read, J., Gu, R.F., Roth, M., Toader, D., Saeh, J.C. and Chen, H. (2013). Mechanism and in vitro pharmacology of TAK1 inhibition by (5 Z)-7-oxozeaenol. *ACS chemical biology*, *8*(3), 643-650.

30. Yu, H., Lee, H., Herrmann, A., Buettner, R., & Jove, R. (2014). Revisiting STAT3 signalling in cancer: new and unexpected biological functions. *Nature reviews Cancer*, *14*(11), 736.

31. Mizuki, M., Fenski, R., Halfter, H., Matsumura, I., Schmidt, R., Müller, C., Grüning, W., Kratz-Albers, K., Serve, S., Steur, C. and Büchner, T. (2000). Flt3 mutations from patients with acute myeloid leukemia induce transformation of 32D cells mediated by the Ras and STAT5 pathways. *Blood*, *96*(12), 3907-3914.

32. Våtsveen, T. K., Sponaas, A. M., Tian, E., Zhang, Q., Misund, K., Sundan, A., Børset, M., Waage, A. and Brede, G. (2016). Erythropoietin (EPO)-receptor signaling induces cell death of primary myeloma cells in vitro. *Journal of hematology & oncology*, *9*(1), 75.

33. Cox, J., Hein, M. Y., Luber, C. A., Paron, I., Nagaraj, N., & Mann, M. (2014). MaxLFQ allows accurate proteome-wide label-free quantification by delayed normalization and maximal peptide ratio extraction. *Molecular & cellular proteomics*, mcp-M113.

34. Tyanova, S., Temu, T., Sinitcyn, P., Carlson, A., Hein, M. Y., Geiger, T., Mann, M. and Cox, J. (2016). The Perseus computational platform for comprehensive analysis of (prote) omics data. *Nature methods*, *13*(9), 731.

35. Tyanova, S., & Cox, J. (2018). Perseus: A Bioinformatics Platform for Integrative Analysis of Proteomics Data in Cancer Research. In *Cancer Systems Biology* (pp. 133-148). Humana Press, New York, NY.

36. Mellacheruvu, D., Wright, Z., Couzens, A. L., Lambert, J. P., St-Denis, N. A., Li, T., Miteva, Y.V., Hauri, S., Sardiu, M.E., Low, T.Y. and Halim, V.A. (2013). The CRAPome: a contaminant repository for affinity purification–mass spectrometry data. *Nature methods*, *10*(8), 730.

37. Subramanian, A., Tamayo, P., Mootha, V. K., Mukherjee, S., Ebert, B. L., Gillette, M. A., Paulovich, A., Pomeroy, S.L., Golub, T.R., Lander, E.S. and Mesirov, J.P. (2005). Gene set enrichment analysis: a knowledge-based approach for interpreting genome-wide expression profiles. *Proceedings of the National Academy of Sciences*, *102*(43), 15545-15550.

38. Mootha, V. K., Lindgren, C. M., Eriksson, K. F., Subramanian, A., Sihag, S., Lehar, J., Puigserver, P., Carlsson, E., Ridderstråle, M., Laurila, E. and Houstis, N. (2003). PGC-1α-responsive genes involved in oxidative phosphorylation are coordinately downregulated in human diabetes. *Nature genetics*, *34*(3), 267.

39. Wu, X., & Karin, M. (2015). Emerging roles of Lys63-linked polyubiquitylation in immune responses. *Immunological reviews*, *266*(1), 161-174.

40. An, L., Jia, W., Yu, Y., Zou, N., Liang, L., Zhao, Y., Fan, Y., Cheng, J., Shi, Z., Xu, G. and Li, G. (2013). Lys63-linked polyubiquitination of BRAF at lysine 578 is required for BRAF-mediated signaling. *Scientific reports*, *3*, 2344.

41. Holderfield, M., Deuker, M. M., McCormick, F., & McMahon, M. (2014). Targeting RAF kinases for cancer therapy: BRAF-mutated melanoma and beyond. *Nature Reviews Cancer*, *14*(7), 455.

42. Rawlins, P., Mander, T., Sadeghi, R., Hill, S., Gammon, G., Foxwell, B., Wrigley, S. and Moore, M. (1999). Inhibition of endotoxin-induced TNF-α production in macrophages by 5Z-7-oxo-zeaenol and other fungal resorcylic acid lactones. *International journal of immunopharmacology*, *21*(12), 799-814.

43. Deng, J., Taheri, L., Grande, F., Aiello, F., Garofalo, A., & Neamati, N. (2008). Discovery of novel anticancer compounds based on a quinoxalinehydrazine pharmacophore. *ChemMedChem: Chemistry Enabling Drug Discovery*, *3*(11), 1677-1686.

44. Grande, F., Aiello, F., De Grazia, O., Brizzi, A., Garofalo, A., & Neamati, N. (2007). Synthesis and antitumor activities of a series of novel quinoxalinhydrazides. *Bioorganic & medicinal chemistry*, *15*(1), 288-294.

45. Thompson, J. E., Cubbon, R. M., Cummings, R. T., Wicker, L. S., Frankshun, R., Cunningham, B. R., Cameron, P.M., Meinke, P.T., Liverton, N., Weng, Y. and DeMartino, J.A. (2002). Photochemical preparation of a pyridone containing tetracycle: a Jak protein kinase inhibitor. *Bioorganic & medicinal chemistry letters*, *12*(8), 1219-1223.

46. Lucet, I. S., Fantino, E., Styles, M., Bamert, R., Patel, O., Broughton, S. E., Walter, M., Burns, C.J., Treutlein, H., Wilks, A.F. and Rossjohn, J. (2006). The structural basis of Janus kinase 2 inhibition by a potent and specific pan-Janus kinase inhibitor. *Blood*, *107*(1), 176-183.

47. Pedranzini, L., Dechow, T., Berishaj, M., Comenzo, R., Zhou, P., Azare, J., Bornmann, W. and Bromberg, J. (2006). Pyridone 6, a pan-Janus–activated kinase inhibitor, induces growth inhibition of multiple myeloma cells. *Cancer research*, *66*(19), 9714-9721.

48. Huang, S. (2007). Regulation of metastases by signal transducer and activator of transcription 3 signaling pathway: clinical implications. *Clinical Cancer Research*, *13*(5), 1362-1366.

49. Murray, M. Y., Zaitseva, L., Auger, M. J., Craig, J. I., MacEwan, D. J., Rushworth, S. A., & Bowles, K. M. (2015). Ibrutinib inhibits BTK-driven NF-κB p65 activity to overcome bortezomib-resistance in multiple myeloma. *Cell Cycle*, *14*(14), 2367-2375.

50. Jiang, J., Ballinger, C. A., Wu, Y., Dai, Q., Cyr, D. M., Höhfeld, J., & Patterson, C. (2001). CHIP is a U-box-dependent E3 ubiquitin ligase: identification of Hsc70 as a target for ubiquitylation. *Journal of Biological Chemistry*.

51. Roux, K. J., Kim, D. I., Burke, B., & May, D. G. (2018). BioID: a screen for protein-protein interactions. *Current protocols in protein science*, *91*(1), 19-23.

52. Zhang, B., Kirov, S., & Snoddy, J. (2005). WebGestalt: an integrated system for exploring gene sets in various biological contexts. *Nucleic acids research*, *33*(suppl_2), W741-W748.

53. Wang, J., Vasaikar, S., Shi, Z., Greer, M., & Zhang, B. (2017). WebGestalt 2017: a more comprehensive, powerful, flexible and interactive gene set enrichment analysis toolkit. *Nucleic acids research*, *45*(W1), W130-W137.

54. Cargnello, M., & Roux, P. P. (2011). Activation and function of the MAPKs and their substrates, the MAPK-activated protein kinases. *Microbiology and molecular biology reviews*, *75*(1), 50-83.

55. Dhillon, A. S., Hagan, S., Rath, O., & Kolch, W. (2007). MAP kinase signalling pathways in cancer. *Oncogene*, *26*(22), 3279.

56. Emuss, V., Garnett, M., Mason, C., & Marais, R. (2005). Mutations of C-RAF are rare in human cancer because C-RAF has a low basal kinase activity compared with B-RAF. *Cancer research*, *65*(21), 9719-9726.

57. Pritchard, C. A., Samuels, M. L., Bosch, E., & McMahon, M. (1995). Conditionally oncogenic forms of the A-Raf and B-Raf protein kinases display different biological and biochemical properties in NIH 3T3 cells. *Molecular and cellular biology*, *15*(11), 6430-6442.

58. Ascierto, P. A., Kirkwood, J. M., Grob, J. J., Simeone, E., Grimaldi, A. M., Maio, M., Palmieri, G., Testori, A., Marincola, F.M. and Mozzillo, N. (2012). The role of BRAF V600 mutation in melanoma. *Journal of translational medicine*, *10*(1), 1.

59. Davies, H., Bignell, G.R., Cox, C., Stephens, P., Edkins, S., Clegg, S., Teague, J., Woffendin, H., Garnett, M.J., Bottomley, W. and Davis, N. (2002). Mutations of the BRAF gene in human cancer. *Nature*, *417*(6892), 949.

60. Pratilas, C. A., Taylor, B. S., Ye, Q., Viale, A., Sander, C., Solit, D. B., & Rosen, N. (2009). V600EBRAF is associated with disabled feedback inhibition of RAF–MEK signaling and elevated transcriptional output of the pathway. *Proceedings of the National Academy of Sciences*, *106*(11), 4519-4524.

61. Larkin, J., Ascierto, P. A., Dréno, B., Atkinson, V., Liszkay, G., Maio, M., Mandalà, M., Demidov, L., Stroyakovskiy, D., Thomas, L. & De La Cruz-Merino, L. (2014). Combined vemurafenib and cobimetinib in BRAF-mutated melanoma. *New England Journal of Medicine*, *371*(20), 1867-1876.

62. Long, G. V., Stroyakovskiy, D., Gogas, H., Levchenko, E., de Braud, F., Larkin, J., Garbe, C., Jouary, T., Hauschild, A., Grob, J.J. & Chiarion Sileni, V. (2014). Combined BRAF and MEK inhibition versus BRAF inhibition alone in melanoma. *New England Journal of Medicine*, *371*(20), 1877-1888.

63. Xie, P., Streu, C., Qin, J., Bregman, H., Pagano, N., Meggers, E., & Marmorstein, R. (2009). The crystal structure of BRAF in complex with an organoruthenium inhibitor reveals a mechanism for inhibition of an active form of BRAF kinase. *Biochemistry*, *48*(23), 5187-5198.

64. Ball, K. A., Johnson, J. R., Lewinski, M. K., Guatelli, J., Verschueren, E., Krogan, N. J., & Jacobson, M. P. (2016). Non-degradative ubiquitination of protein kinases. *PLoS computational biology*, *12*(6), e1004898.